



**US Army Corps  
of Engineers**  
Kansas City District

---

# Lower Missouri River Sediment Model Calibration Report

---



JULY 2018

## 1.0 Introduction

The bed of the Missouri River experiences both short-term fluctuations, episodic responses to major floods, and long-term trends (USACE 2017a). Effective long-term management of the river should acknowledge and incorporate the effects of these bed elevation changes. This document serves as an initial orientation to development of a mobile-bed sediment model for the lower 500 miles of the Missouri River. Hereafter this model is referred to as the Lower Missouri River Sediment Model (LMRSM). The model creation and calibration followed the basic principles outlined in the HEC-6 Calibration Guide (HEC 1982) and EM 1110-2-4000, with some adaptation. This document summarizes river behavior and provides information on the model set up and calibration.

The purpose of the LMRSM is to compare future bed elevations under alternative management scenarios. The immediate purpose is to provide a 2033 bed elevation projection for use in the Missouri River Recovery Program under the various proposed alternatives. This is a planning level model to assess the reach and river scale effects of proposed alternatives. Final design of habitat projects will require additional calculations or modeling beyond the output of this mobile-bed model.

This report covers model development and calibration. A subsequent report will document alternatives testing.

## 2.0 River Behavior

### 2.1 River History and Modifications

The Missouri River in its current form is a highly regulated, highly stabilized river that drains approximately 529,350 square miles (USACE 2006). Major tributaries include the Yellowstone River, the Platte River, and the Kansas River, each of which drains more than 60,000 square miles. Prior to channel modification, the Missouri River was a wide, braided channel which occupied approximately 300,000 acres downstream of Sioux City, IA. Through the construction of a series of river training structures (dikes and revetments), the river was transformed into a single-thread channel with projected surface area of 112,000 acres (USACE 1981) downstream of Sioux City, IA. The current river is significantly narrower than the original, pre-modified river.

The system of river training structures is called the Bank Stabilization and Navigation Project (BSNP). Structures that run parallel to the river are called revetments, while those that protrude into the river are commonly called dikes. The dikes are generally several hundred feet to over a half mile long, but many of the dikes have most of their length buried in accreted land so that only a small portion of each dike is actually exposed to flow. Most dike structures downstream of Rulo, Nebraska are extended by a low sill which protrudes further into the channel. In common usage, the entire structure, both dike and sill, is

referred to as a dike. Figure 1 illustrates a dike structure with a low sill with typical dimensions in reference to the CRP (Construction Reference Plane). The CRP is a sloping datum mirroring the water surface profile exceeded 75% of the time during navigation season, and is used to set structure heights to overtop at consistent frequencies based on design criteria from December 1973. A more detailed history of BSNP structure design standards, modifications, and current condition is included in the Missouri River Bed Degradation Feasibility Study report.

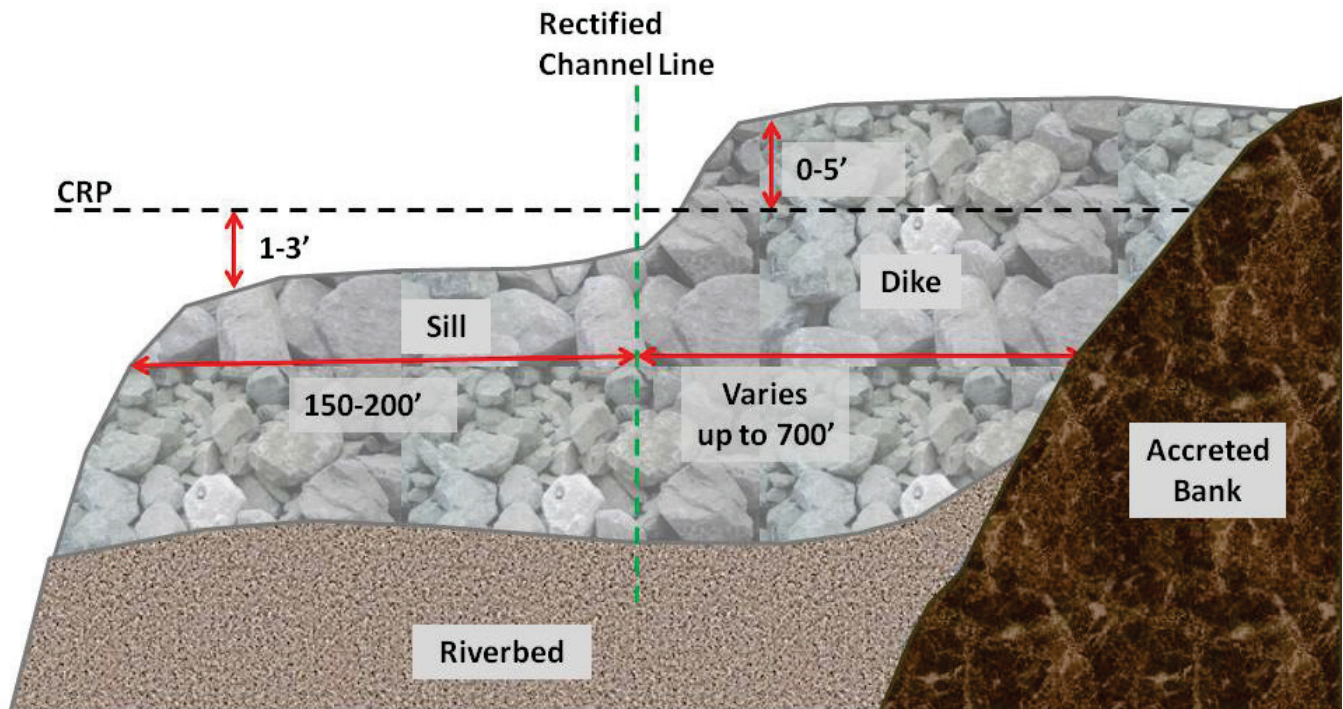


Figure 1. BSNP Dike and Sill with Typical Dimensions, not to scale

In conjunction with the BSNP, a series of six mainstem dams were constructed. These dams store a significant volume of water, reducing downstream flooding and supplying water to support navigation on the lower Missouri River eight months out of the year. The authorized purposes for the Missouri River Mainstem Reservoir System as outlined in the Section 9 of the 1944 Flood Control Act include: flood control, navigation, irrigation, hydropower, water supply, water quality control, recreation, and fish and wildlife (USACE 2006).

The channel stabilization accomplished through the BSNP has allowed the construction of miles of federally operated and maintained levees and floodwalls and additional privately owned levees generally located on both banks of the Missouri River downstream of Omaha, Nebraska. Portions of these levees, particularly in the more urbanized areas, as well as smaller privately owned agricultural levees, are located immediately adjacent to the river bank. At many locations, these small, privately-owned levees contain flows with a 5 to 10-year return interval at top width only slightly larger than the channel. Larger floods exceeding a 50-year return period are generally only contained by the federally

constructed levees and only a few private levee systems. Due to the varying levels of protection of these levees, channel widths for major floods vary considerably from location to location (see Figure 2.)

Figure 2 graphically depicts the level of confinement imposed on the river corridor by levees vs. the natural floodplain width. The widths shown in Figure 2 were developed using existing models not the ManPlan study model. The “Valley Width” line in Figure 2 indicates the floodplain width for the 1% AEP profile if there were no levees and is provided as a reasonable approximation for the valley width. Figure 2 is not used in the sediment modeling, but is provided for context to differentiate geologic constrictions from levee-induced constrictions. The LMSM includes the levees at the actual locations.

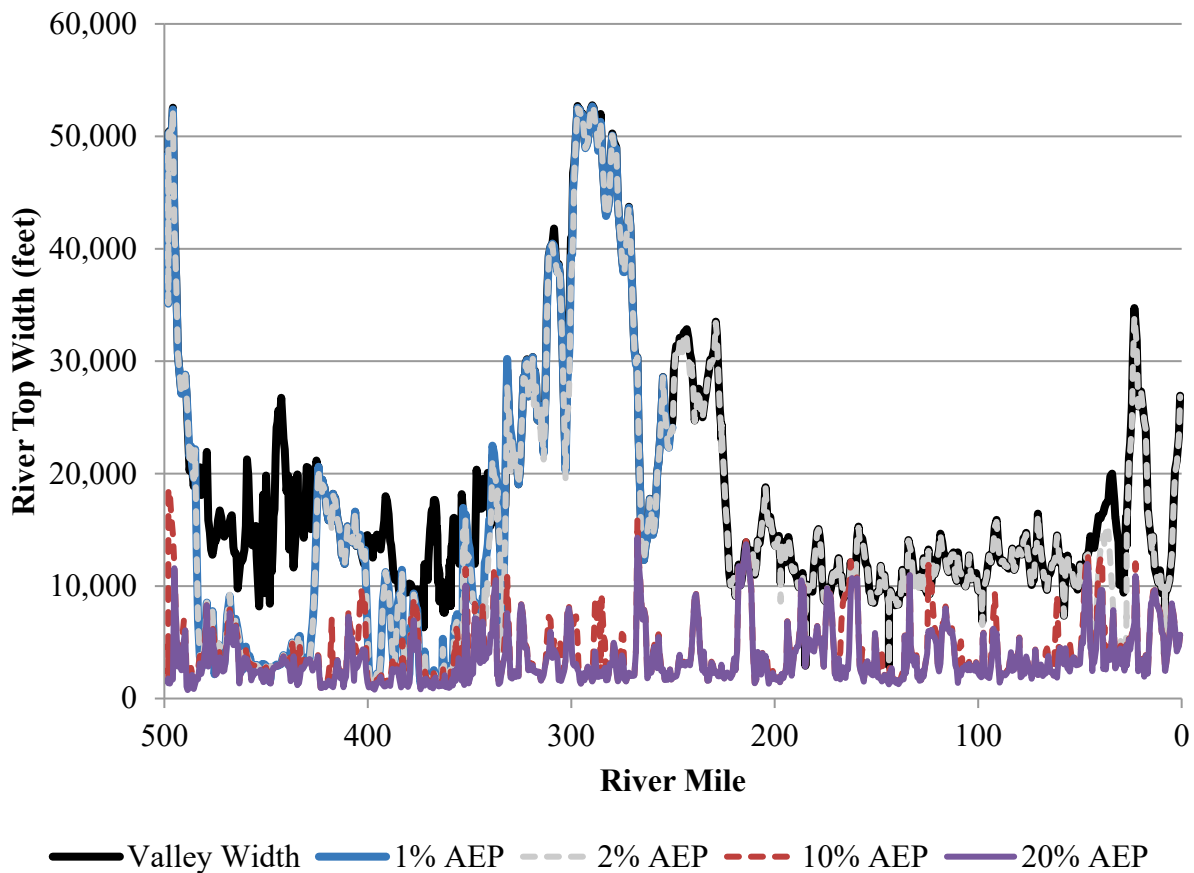


Figure 2. Valley Width and River Top Width at Different Flood Levels

There are no man-made grade controls on the lower Missouri River downstream of Gavin’s Point Dam which is located at RM 811. Riprap placed at bridge piers does not armor the entire bed and has not stabilized the river. There are no known natural grade controls in the active channel, though this has not been the subject of a thorough investigation. There are some natural bedrock outcroppings on the river banks (Laustrup et al. 2007). The stability of the river near Waverly may be due to natural rock outcropping at that location, but may be caused by other factors. Borings at bridge locations indicate 40 to 100 ft of sand to bedrock in the Kansas City Reach (MoDOT 2008).

## 2.2 Sediment Loads

The sediment load in the Missouri River is quite variable, with high flows typically carrying exponentially more sediment than low flows. USACE (2017a) notes that the historic flood of 1993 brought about a downward shift in the flow-sediment relationship at the St. Joseph gage. The exact cause of this phenomenon is not known, but may be due to the deposition of bed material on the floodplains leading to less in-channel sediments available for transport (Horowitz 2006). This was a temporary phenomenon, however, and not a trend. As seen in Figure 3, sediment loads after 1993 were within the scatter of the sediment loads from 1952 – 1992. During the 2011 flood, the flow-load relationship temporarily decreased, which can be explained by the high volumes of clear water which came from the upstream reservoirs. It appears that for low flows, the post-2011 sediment levels are lower than pre-flood (but within the pre-1993 scatter), but for moderate flows, the flow-load relationship has returned to pre-2011 levels.

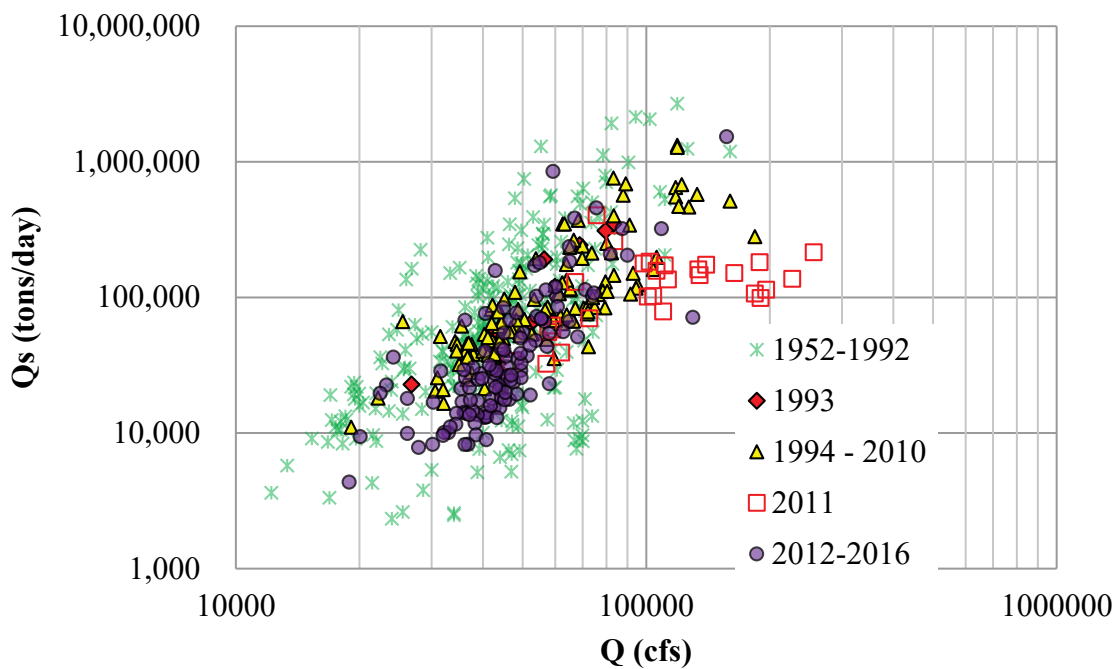


Figure 3. Sediment load at the St. Joseph, MO gage.

## 2.3 Commercial Dredging

The bed of the Missouri River is dredged (mined) downstream of Rulo, Nebraska as a source of sand and gravel. Commercial dredging on the Missouri River has taken place for many years to varying amounts. Historically, most of the extraction from the bed of the Missouri River took place in the Kansas City metro area, with additional operations in St. Joseph, Waverly, Jefferson City, and St.

Charles. Figure 4 shows the extracted quantities for the Missouri River from 1935 to 2016. As seen, the total dredging take began increasing in the 1950s. It increased sharply in the early 90s and remained high through the 2000s. This sharp increase was a result of regulatory restrictions on dredging on the Kansas River and increased local demand for construction materials. The level of dredging in 2002 includes USACE dredging for the construction of the L-385 unit of the Federal Missouri River Levee System. The annual extraction began falling in the late 2000s and is now around 4 million tons per year. Commercial sand and gravel dredging removed a total of approximately 247 million tons (181 million yd<sup>3</sup>) from the bed of the lower 500 miles of Missouri River from 1935 to 2016. USACE (2017a) concludes that commercial sand and gravel dredging was the dominant cause of bed degradation from St. Joseph to Waverly, MO from 1994 to 2014.

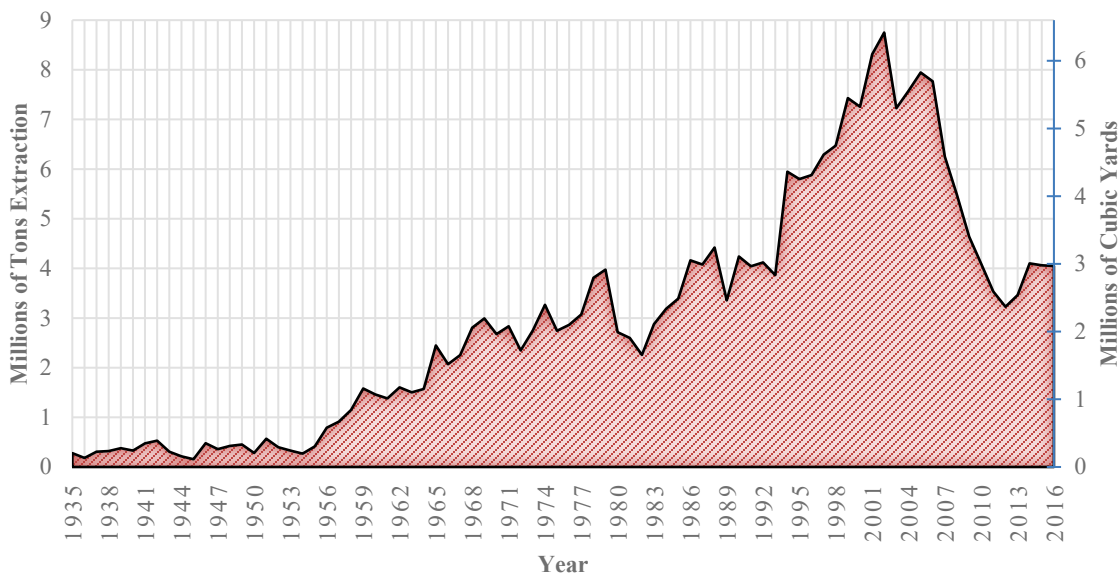


Figure 4. Extracted Dredging Quantities for the Missouri River in Kansas City

#### 2.4 Stage and Low Water Surface Profile Degradation

The lower Missouri River has experienced significant bed degradation – persistent lowering of the river bed (USACE 2017a, 2011, 2009). Bed degradation of the Missouri River has caused a corresponding though not necessarily equivalent drop in the water surface elevations for low discharges. Figures 5, 6, 8, and 9 demonstrate that the stage of low discharges has been dropping at St. Joseph, Kansas City, Boonville, and Hermann gages, respectively (USACE 2017b). At the Waverly gage (Figure 7) the low stages have been relatively stable.

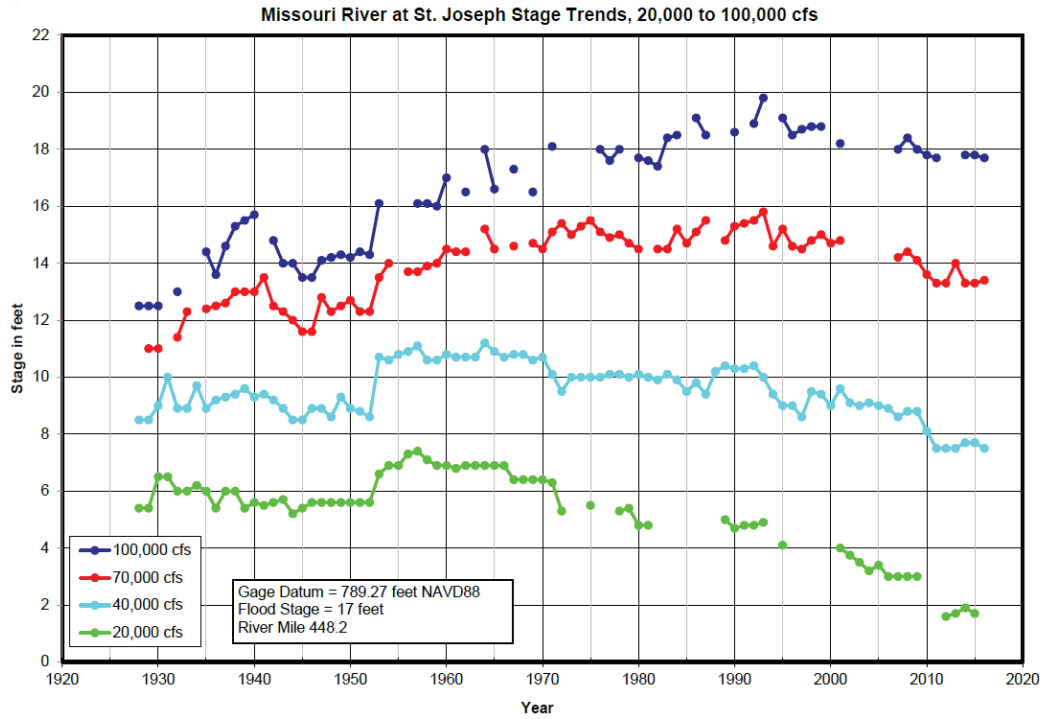


Figure 5. Missouri River Stage Trends- Missouri River at St. Joseph, MO

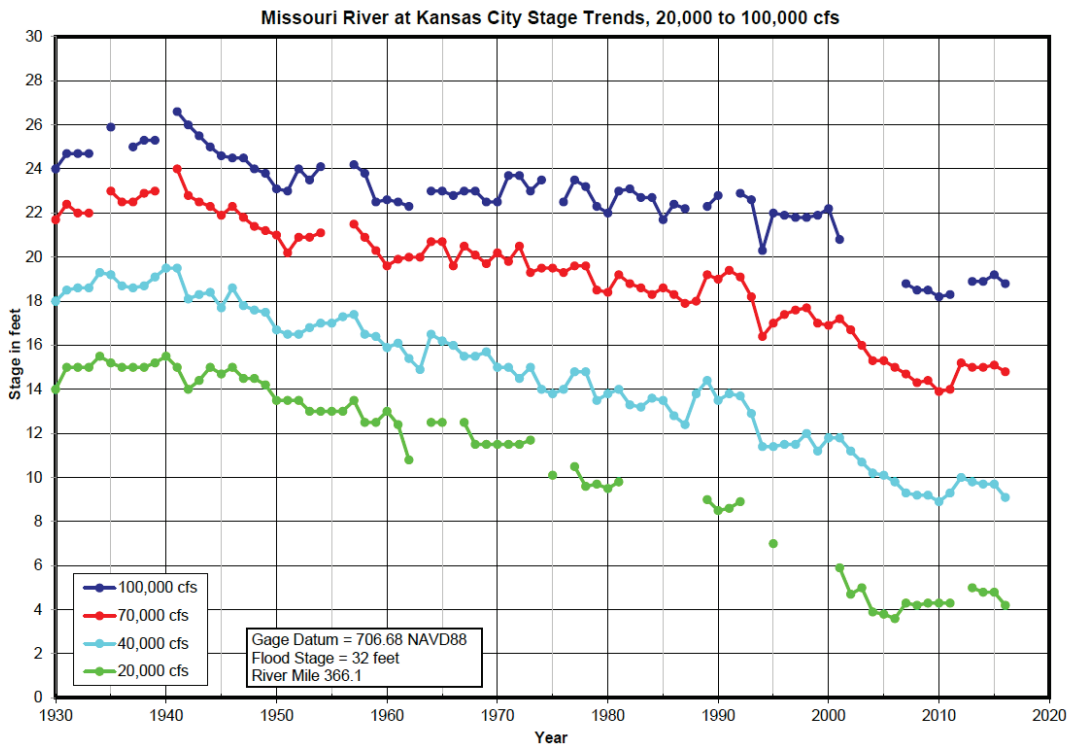


Figure 6. Missouri River Stage Trends- Missouri River at Kansas City, MO

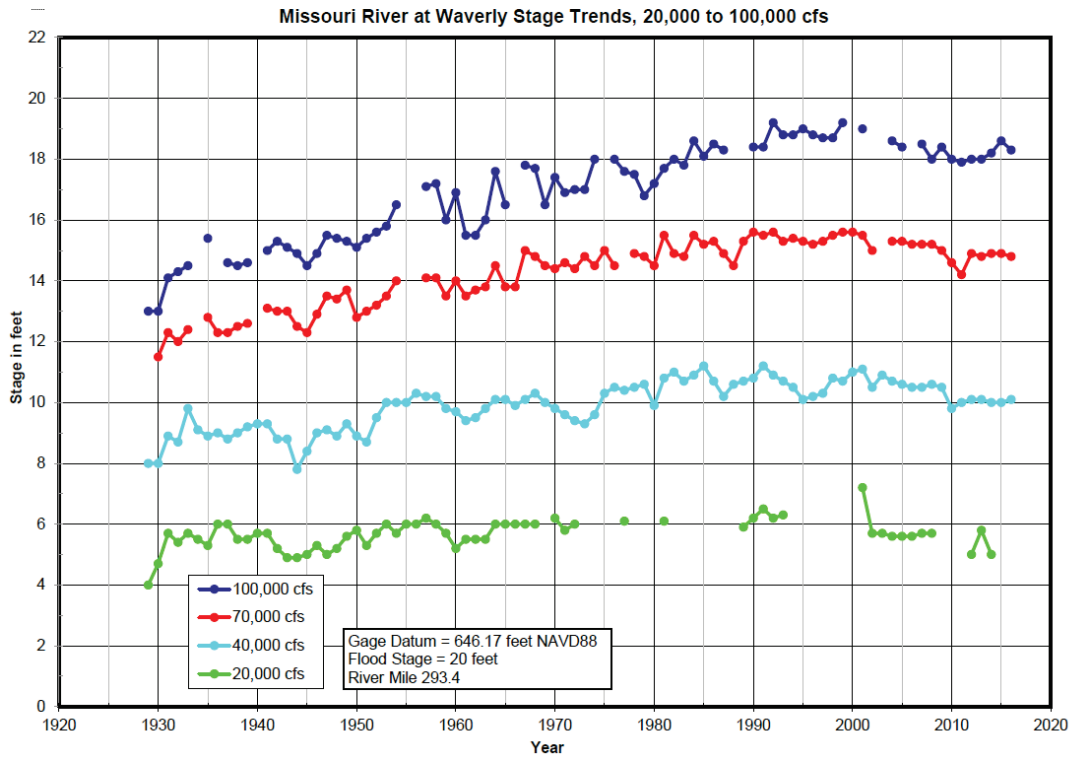


Figure 7. Missouri River Stage Trends- Missouri River at Waverly, MO

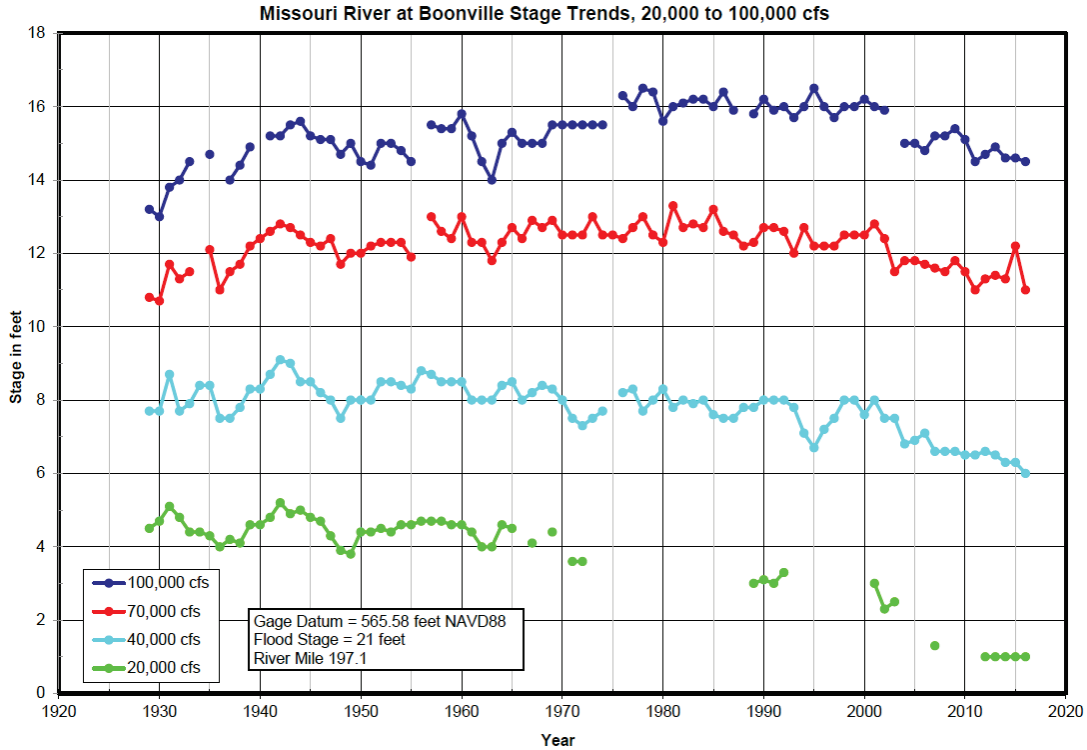


Figure 8. Missouri River Stage Trends- Missouri River at Boonville, MO

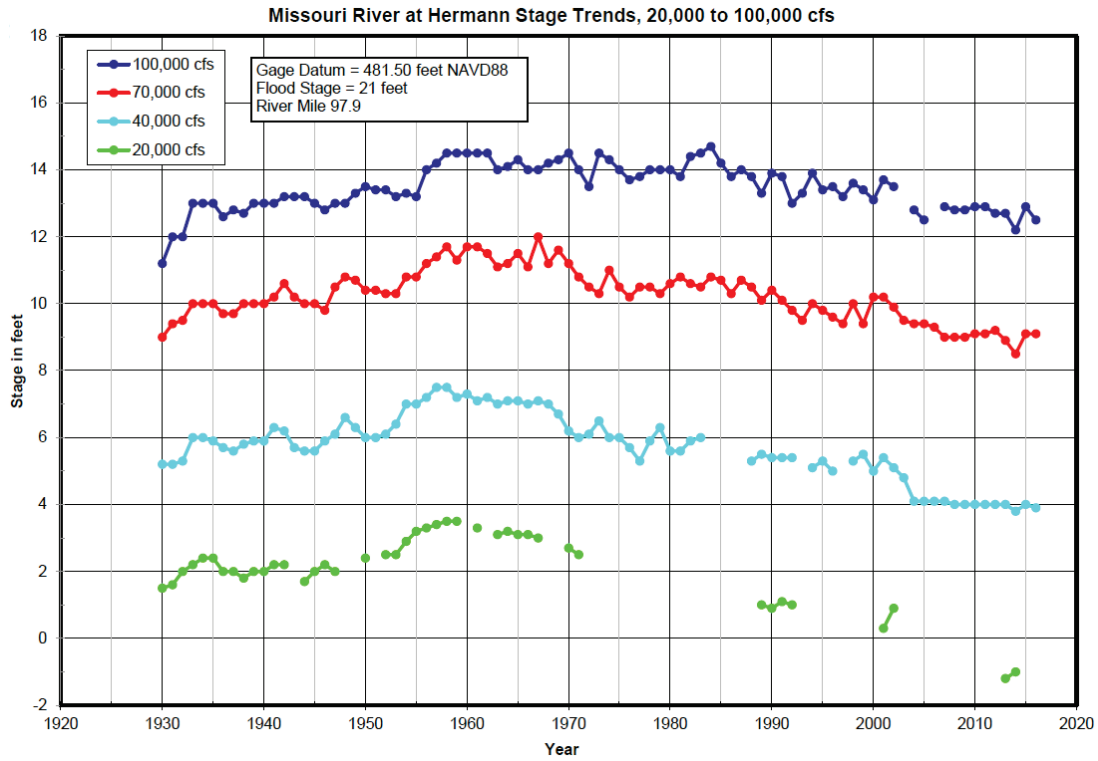


Figure 9. Missouri River Stage Trends- Missouri River at Hermann, MO

On the lower Missouri River, water surface elevations at dozens of locations have been measured on an annual or biannual basis for decades, which provided a way to track stage trends over time for the full lower 500 miles. These low water profiles were measured when flow rates were within a tight range, and then were adjusted to a consistent discharge based on rating curves at nearby gages to allow valid comparison (USACE 2010). Figure 10 plots selected profiles from 1974 to 2017 as a change compared to the average slope of the river. The average slope is defined by the starting and ending elevations of the 2010 Construction Reference Plane.

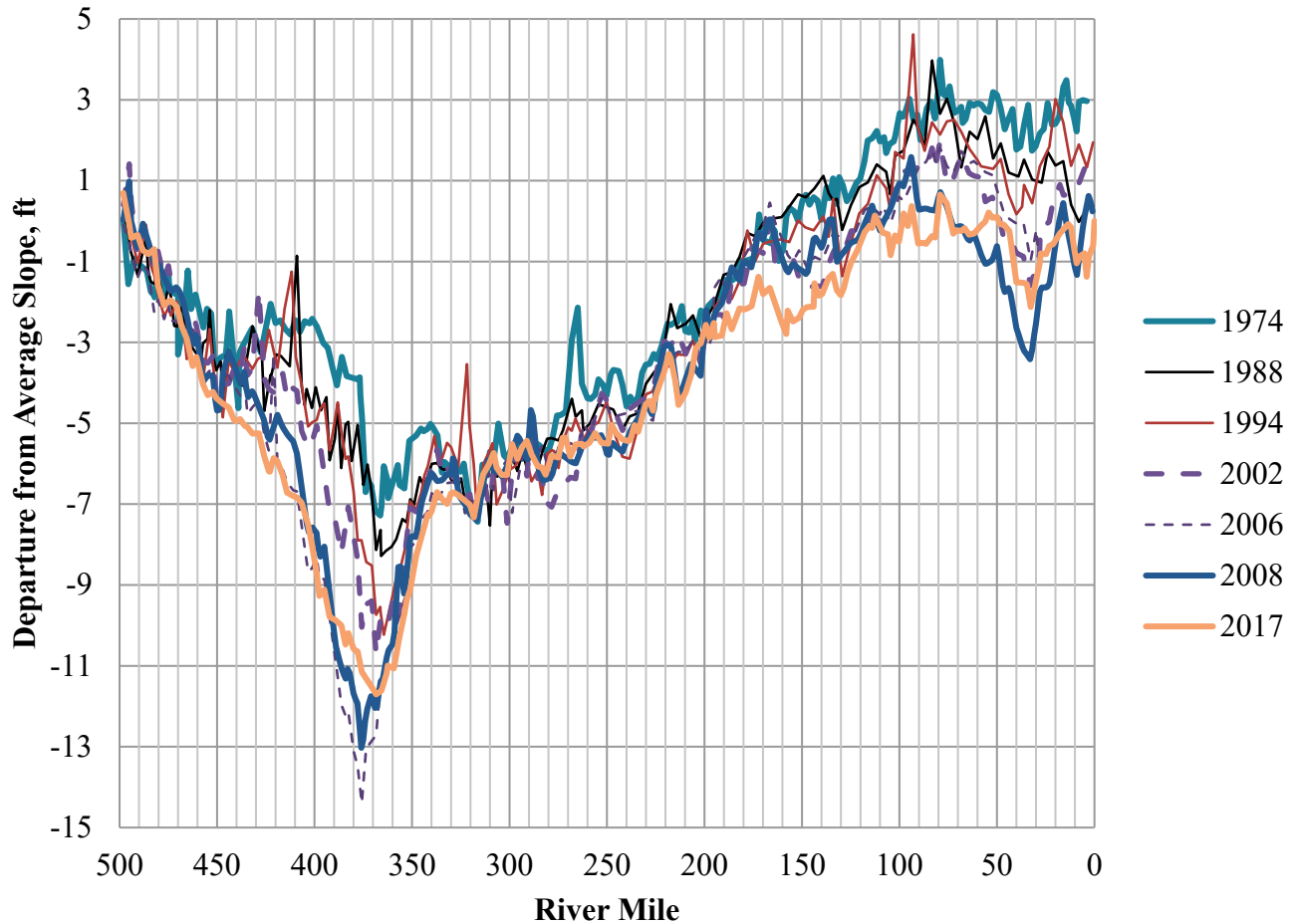


Figure 10. Low Water Surface Profiles—Departure from Average Slope

The rates of low water surface degradation vary considerably over the 500 miles. In some stretches of the river, degradation is insignificant, while in other areas, degradation has already induced damage to the BSNP and federal levee system, and necessitated expensive repairs and retrofits of other public and private infrastructure (USACE 2017a). As seen in Figure 10, areas of localized depression existed as of 1974 in the Kansas City metro area (RM 350 to 380). Very significant degradation has occurred since 1974, especially RM 450 to 320 and 200 to 0.

## 2.5 Bed Elevation and Volume Changes

Figure 11 presents the average bed elevations for key survey years, averaged over 5-mile reaches. As in Figure 10, the elevations are spatially de-trended (i.e. what is plotted is the departure from the average river slope) to allow easier visual comparison among years. The average river slope is computed by drawing a linear trend line from the average elevation in the most upstream 5 miles to the average elevation in the most downstream 5 miles.

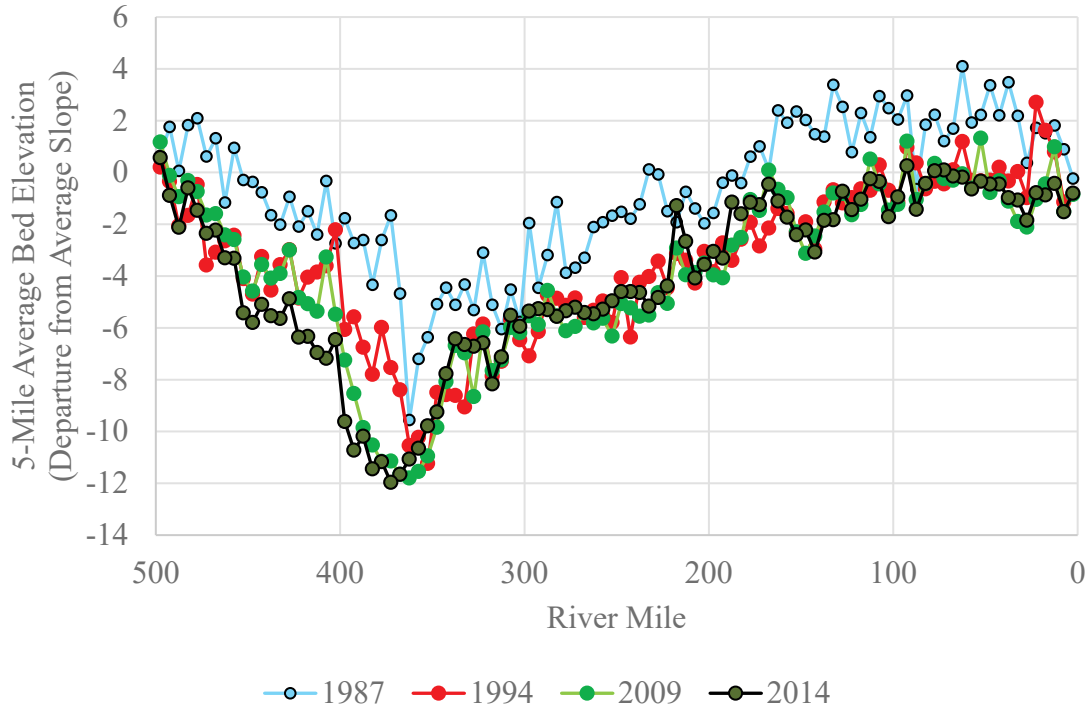


Figure 11. Spatially De-trended Average Bed Elevations (5-Mile-Average Departure from Average Slope)

As seen in Figure 11, very significant bed lowering occurred between the 1987 and 1994 surveys, which can be attributed predominantly to the effects of the 1993 flood. After 1994, the bed continued to degrade from approx. RM 360 to 450. Numerical modeling in USACE (2017a) indicates that further degradation after 1994 from RM 360 to 390 was induced by commercial dredging and that this degradation migrated upstream as a result of the 2011 flood. The scatter precludes visual identification of trends downstream of RM 360 using Figure 11. These trends can be seen in the longitudinal cumulative volume change curves between each consecutive set of surveys, as presented in Figure 12. On longitudinal cumulative volume change curves, a downward slope indicates degradation, while an upward slope indicates recovery.

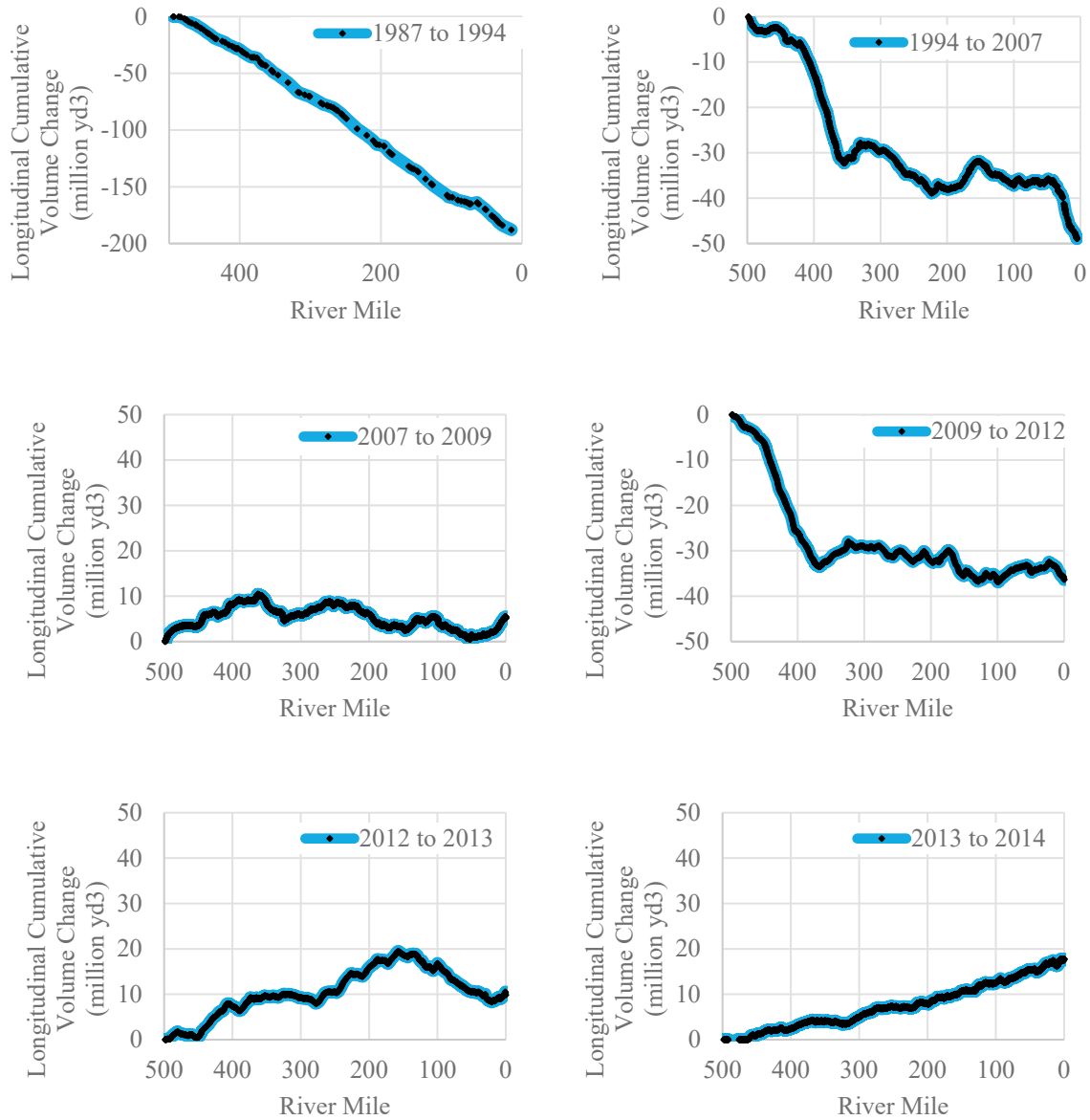


Figure 12. Longitudinal Cumulative Volume Change Between Successive River-Wide Surveys. Note the different scale for the 1987 to 1994 change.

The 1993 flood, which produced discharges of over 540,000 cfs in Kansas City (RM 366.2) caused tremendous degradation on the lower Missouri River. As seen in Figure 12, the Missouri River degraded 187.9 M yd<sup>3</sup> from 1987 to 1994. Commercial dredging over the same time period totaled 22.8 M yd<sup>3</sup>, indicating that 165.1 M yd<sup>3</sup> was caused by an imbalance in sedimentation processes (i.e. the sediment leaving the lower Missouri River exceeded the sediment entering). As discussed later in this report, this sediment most likely deposited on the floodplain.

Following the 1993 flood, from 1994 to 2007 the river degraded an additional 48.9 million yd<sup>3</sup>. Channel mining during this time period totaled 69.5 million yd<sup>3</sup>, indicating that the channel mining prevented what would have been a bed recovery trend of 1.6 million yd<sup>3</sup> / year. The 2007 to 2009 analysis indicates localized degradation and aggradation with overall aggradation of 5.1 million yd<sup>3</sup>.

From 2009 to 2012, the river degraded an additional 36.4 million yd<sup>3</sup>, principally as a result of the 2011 flood. In Kansas City during the 2011 flood, the flow remained above 142,000 cfs (a 2-year flow) for over 100 days, which was approximately 40 days longer than the record flood of 1993. Upstream of RM 367, the degradation profile from the 2011 flood closely matches that of the 1993 flood. Downstream of RM 367, the bed degraded during the 2011 flood, but not nearly as much as in 1993.

Following the 2011 flood, from 2012 to 2013 the river recovered from RM 500 to 160 but continued to degrade from RKM 160 to 0, with a river-wide net recovery of 9.8 million yd<sup>3</sup>. From 2013 to 2014 the river responded much more uniformly, recovering 17.8 million yd<sup>3</sup>.

Overall, from 1987 to 2014, the bed of the river for the lower 500 miles of Missouri River degraded approximately 240 M yd<sup>3</sup>, computed as the sum of the volume change between each successive set of surveys. Figure 13 indicates the components that sum to this quantity of total bed degradation. The “1993 Flood” component is the bed change seen from 1987 to 1994 minus the dredging over the same time period. The “2011 Flood” component is the bed change from 2009 to 2012 minus the dredging over the same time period. The dredging component is the sum of reported dredging tonnages from 1987 to 2014, converted to a volume. The “Natural Recovery Rate” component was found by subtraction and represents the level of rebound that could have occurred over this time period without direct removal of bed sediment via dredging. These volumes are specific to the 1987 to 2014 time period, which are not necessarily reflective of future bed change or average natural sediment recovery rates.

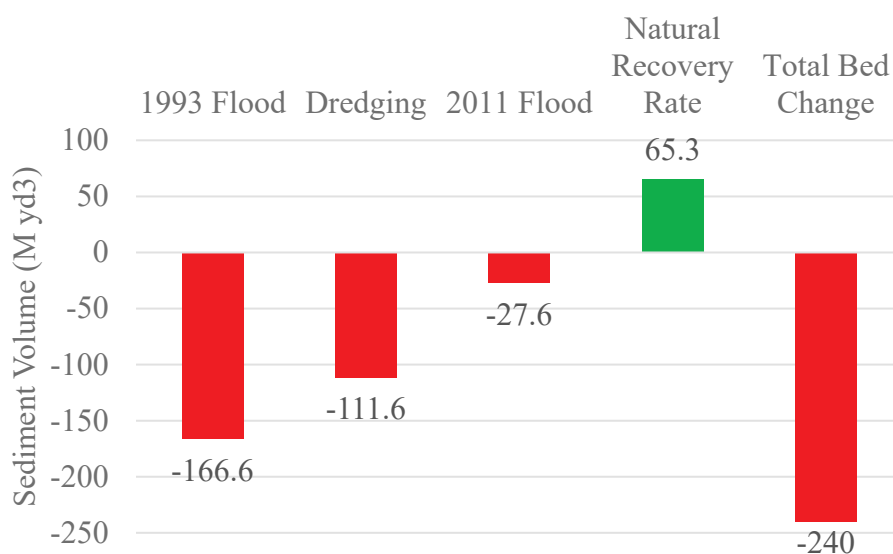


Figure 13. Components of Bed Change from 1987 to 2014

## **3.0 Model**

### **3.1 Model Introduction**

A HEC-RAS 5.0.3 sediment model was developed to predict differences in future bed elevation trends among alternatives. The model runs from RM 498.1, near Rulo, NE to RM 0.74 near the confluence with the Mississippi River. There are 801 cross sections with median spacing of 3354 ft (ranging from 671 ft to 6921 ft.) This resolution allows testing of reach-scale effects.

### **3.2 Model Schematic**

Figure 14 provides a schematic of the model network with river miles, major tributaries, channel cross-sections, and USGS gages located. Due to the length of the river modeled, a detailed mapping of all pertinent features including levees, floodwalls, and river training structures for the full 500 river miles is not provided here. The reader is advised to review the Missouri River Hydrographic Survey Mapbook (USACE 2004).

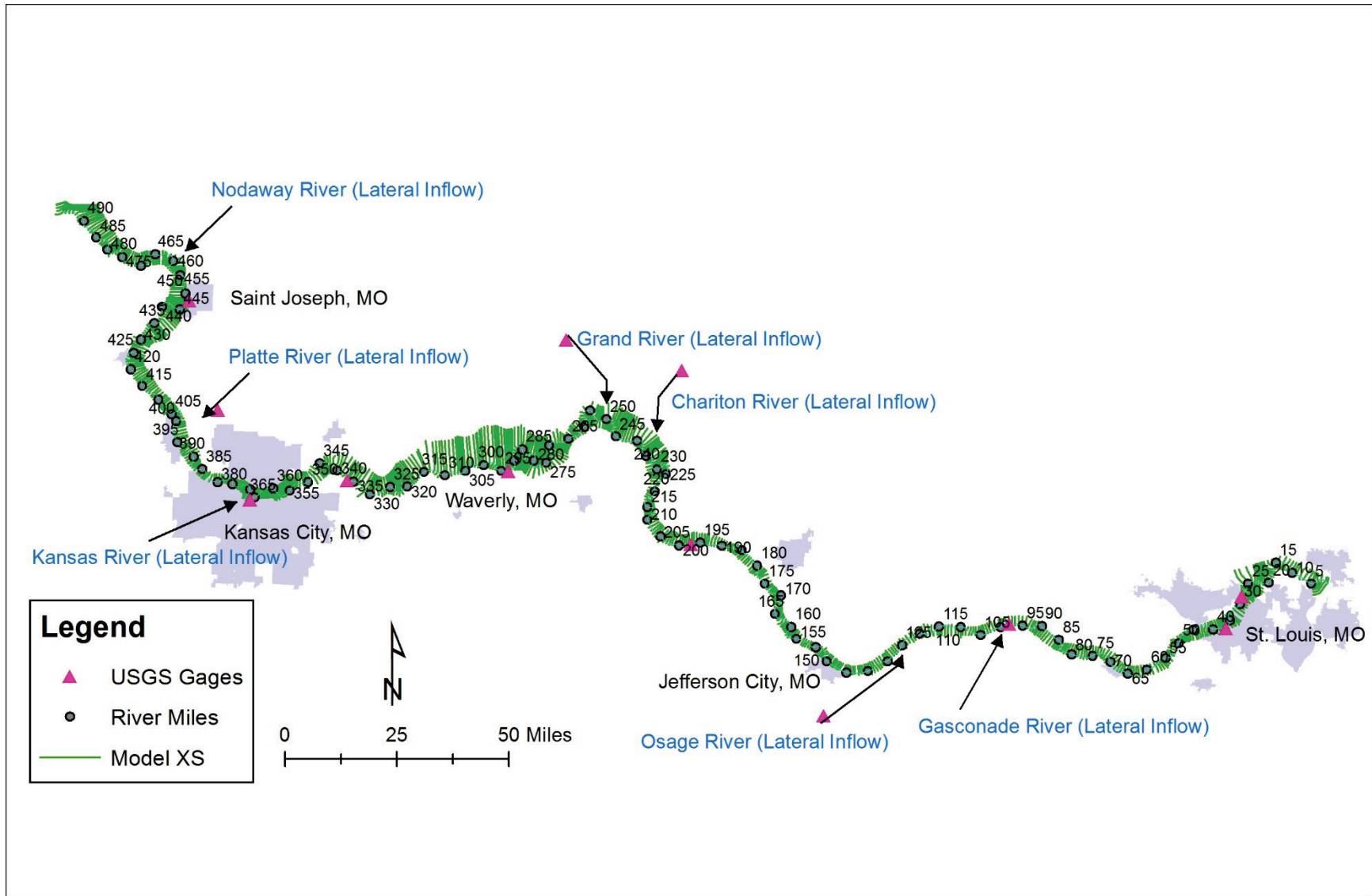


Figure 14. Model Schematic

### 3.3 Initial Conditions

Initial channel conditions consist of cross-sections, roughness values, and lateral extent, depth, and gradation of the bed. These initial conditions are described in the following paragraphs.

#### **Cross-Sections**

The starting geometry was synthesized using bed bathymetry from the 1994 hydrographic survey data (USACE 1994) and bank and overbank data from 2013 LIDAR. The model cross sections were chosen to generally match the locations of the floodway model, with consideration for the locations of the 1994 data. The cross-sections utilize the Missouri River 1960 river mile nomenclature. However, reach lengths are based on the actual channel distance between cross-sections along the sailing line, which varies slightly from using a difference in river miles to compute lengths. The starting year of 1994 was chosen due to data availability; a full hydrographic survey was conducted in 1994 which documented bed elevations as well as dike and revetment geometry. Not all cross-sections present in the 2007 floodway model were retained in the degradation model. Cross-sections with unrealistically small or large cross-sectional areas, cross-sections that were too tightly spaced and bridge cross-sections were removed to achieve model stability.

Dike, sill, and revetment structures were entered into the cross-sections as station/elevation points to account for the blocked flow area between dike structures. The methodology is similar, but more robust, to that used on the Missouri River by Teal and Remus (2001) and in USACE (2017a). Conceptually, the ineffective flow areas within each control volume are summed, then divided by the control volume length in order to compute the blocked area to be entered into each cross section. Figure 15 conceptually displays the process. Figure 16 displays actual computed data for the same river location.

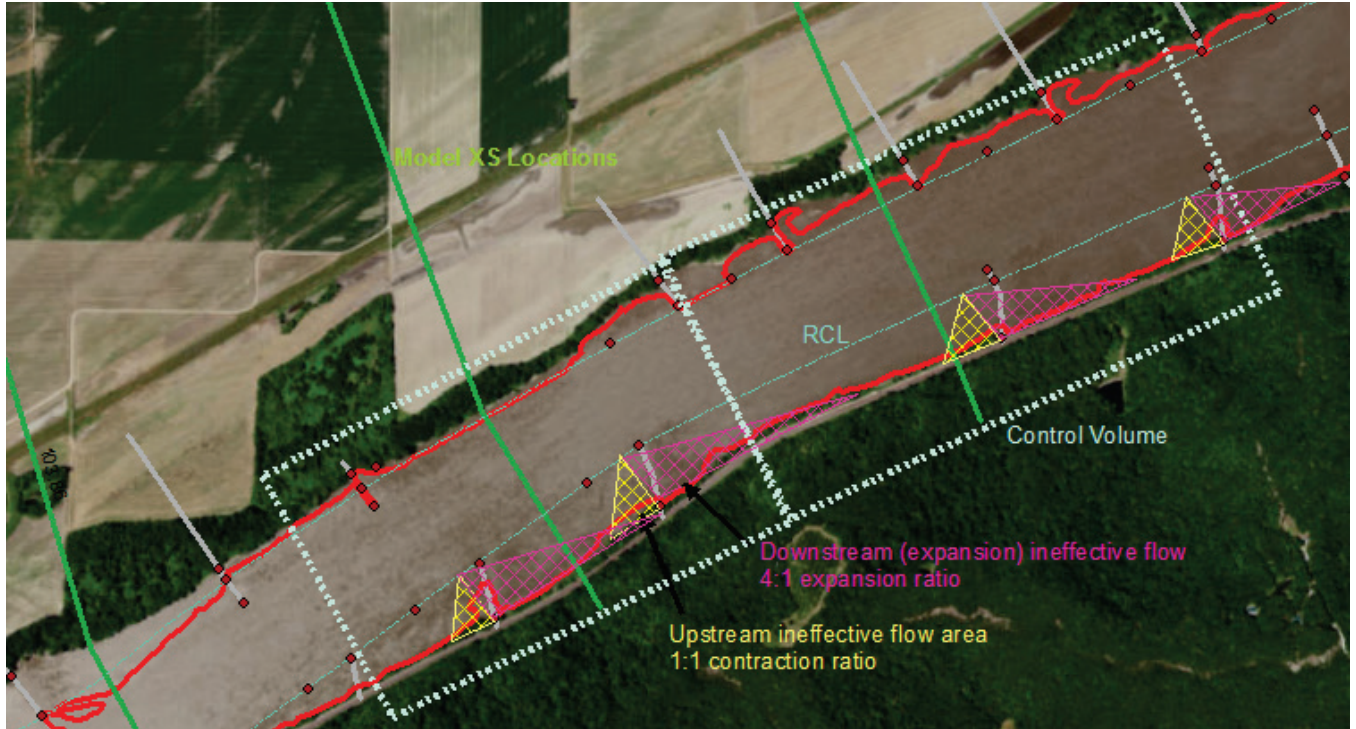


Figure 15. Conceptual depiction of ineffective flow areas from dike structures

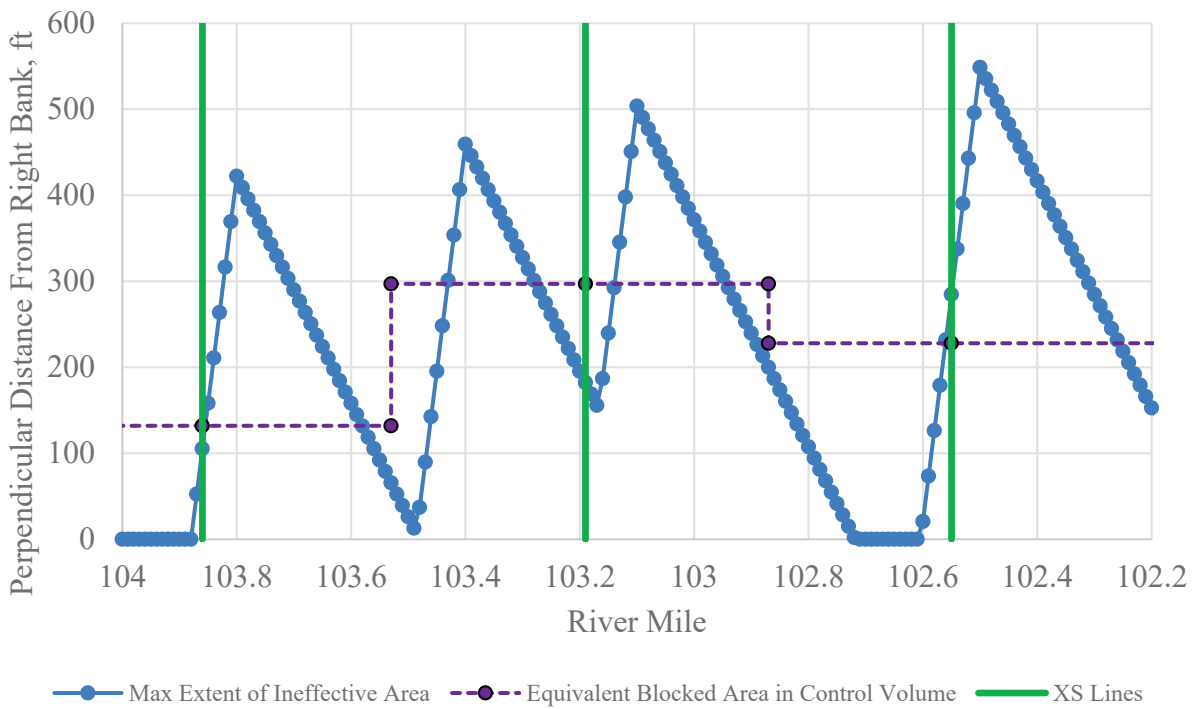


Figure 16. Computation for effective dike length

The following steps summarize the process:

1. Structures in the GIS layer representing dikes and sills were assigned to either the right or left bank.
2. The perpendicular length of each dike structure was found using GIS. This was accomplished by computing the intersection point of each dike structure with a GIS layer representing the low bank, then finding the shortest distance between that intersection point and the Rectified Channel Line. Distances for locations where a dike intersected a bank more than once and other anomalies were manually measured in ArcMap or GoogleEarth.
3. The perpendicular length of each sill structure was assumed equal to the GIS line distance for the portion of structure riverward of the Rectified Channel Lines.
4. The remaining steps were executed four times. Once for the dike structures (structure length as described in step 2) and once for the sill structure (structure length = dike length as in step 2 + the sill length as in step 3). Then repeated twice more for the dikes and sills on the opposite bank.
5. For each hundredth-mile increment from RM 497.7 to RM 0.49, the maximum riverward extent of the ineffective flow area of the bounding dikes was calculated. The zone of expansion was assumed to be 4:1 on the downstream end of each dike. The zone of contraction was assumed to be 1:1 on the upstream end of each dike. The closest bounding dikes did not necessarily generated the most riverward extent of ineffective flow; closer, shorter dikes were at times in the shadow of slightly more distant, longer dikes. To remedy, the ineffective flow expansion/contraction line for four dikes upstream and two dikes downstream of each increment were considered and the maximum length of ineffective flow selected. See Figure 16.
6. The total ineffective flow area was computed for each control volume, then divided by the length of the control volume to yield an effective dike length.
7. This effective dike length was entered into the HEC-RAS model as a blocked obstruction then converted to sta/elev points.

Structures extending from the channel bank to the Rectified Channel Line were assigned the elevation criteria for a dike (the average of the concave and convex design elevations).

Structures from the rectified channel line and further into the channel were assigned the design criteria for a sill. These criteria are provided in Table 1. The 1982 CRP, which was the official CRP in use in 1994, was used to set the structure elevations. L-head revetment heights were read individually from the 1994 Missouri River Hydrographic Survey Mapbook (USACE 1994).

Table 1. Dike and Sill Elevations in Model

River Mile Range	Offset from 1982 CRP (ft)			
	Concave Dike Criteria	Convex Dike Criteria	Model Dike Elevation	Sill (Criteria and Model)
498 to 367	+3	+1	+2	-2
367 to 250	+3	+1	+2	-2
250 to 130	+4	+2	+3	-2
130 to 0	+5	+3	+4	-1

As this is a quasi-unsteady, not truly unsteady flow model, levee breaches were not modeled. As RAS allows only one levee point in each overbank, smaller levees were typically included as ineffective flow areas and larger levees as levee points. The levees were placed to maintain an accurate distance between the river bank and the levee, as measured in GIS from the National Levee Database shapefile. The simplified treatment of levees inherent to a quasi-unsteady flow model limits the ability of this model to predict flood heights or floodplain deposition during extreme (levee overtopping) events.

In quasi-unsteady flow modeling, a levee that is overtopped instantly and fully contributes to the flow (i.e. there is no time factor for filling and draining). Where this was problematic, additional permanent ineffective flows were added. Ineffective flows were also included to bridge over chutes present in the LIDAR that were not constructed until later in the calibration period and to fill in the area behind L-head revetments.

**Roughness**

Channel roughness was assigned as Manning ‘n’ values in four horizontally-varied regions: the active channel (n = 0.028), the channel with sill influence (n = 0.041), the channel with dike influence (n = 0.0413), and the floodplain (n = 0.07). These regions are delineated in Figure 17. Variations in roughness among large reaches were included in the flow-roughness change factors, listed in Table 2, rather than in the base level ‘n’ values. Lisbon chute began flowing in 1996 and was assigned an ‘n’ value of 0.05. Cranberry bend was present prior to 1994 and was assigned an n value of 0.029. The remainder of the chutes were not constructed until late in the calibration period and were assigned the floodplain ‘n’ value of 0.07.

Measured water surfaces at the Kansas City gage indicate that at very high flows, the roughness for the active bed decreases as the bed transitions from dunes to plane bed. This was physically verified using multi-beam bathymetric surveys, as documented in USACE (2017a). Table 2 presents the flow-roughness values used in the model.

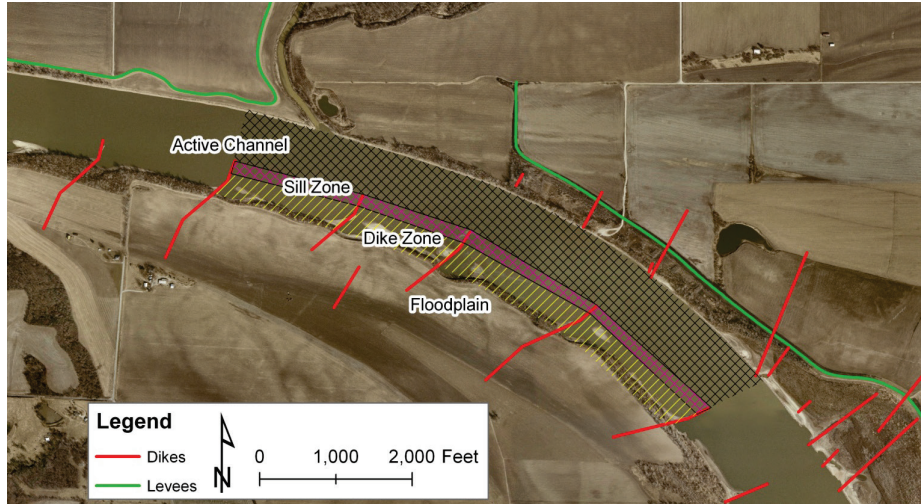


Figure 17. Active Channel and Inter-dike Regions

Table 2. Flow-Roughness Change Factors

RM 498.1 to 463.97	
Q (cfs)	Roughness Factor
0	1.05
70000	1.05
120000	1
150000	0.95
200000	0.92

RM 463.17 to 393.18	
Q (cfs)	Roughness Factor
0	1.09
50000	1.09
70000	1.05
120000	1
150000	0.95
200000	0.9

RM 392.59 to 367.89	
Q (cfs)	Roughness Factor
0	0.95
70000	0.95
120000	0.85
200000	0.8

RM 367.57 to 321.11	
Q (cfs)	Roughness Factor
0	1
50000	1
70000	0.98
120000	0.98
150000	0.95
200000	0.9

RM 320.42 to 250.85	
Q (cfs)	Roughness Factor
0	1.02
50000	1.03
120000	1.03
150000	1.02

RM 250.23 to 169.13	
Q (cfs)	Roughness Factor
0	0.9
70000	0.9
120000	0.9
150000	0.85

RM 62.92 to 0.774	
Q (cfs)	Roughness Factor
0	1
70000	1
120000	0.95
150000	0.95

### Tributaries

Seven major tributaries enter the Missouri River in the model reach: the Nodaway River (RM 463.17), Platte River (RM 391.29), Kansas River (RM 367.57), Grand River (RM 250.23), Chariton River (239.32), Osage River (RM 130.37), and Gasconade River (104.49). Over the calibration period (1994 – 2014) the combined flow inputs from these tributaries totals aprx. 31% of the flow in the Missouri River at St. Charles, MO. These tributaries were included as flow and sediment boundary conditions. As explained later, the differences in flow and sediment at the mainstem gages beyond those explicitly specified are included as uniform lateral flows. Thus the flow and sediment inputs from other tributaries such as the Big Nemaha, Lamine / Blackwater, etc. are included in these uniform lateral flow and sediment inputs.

### Bed Sediment Extent

The moveable bed limits were initially set at the toe of the most riverward structure (dike or sill). These limits were adjusted as needed for model stability or calibration. The depth of the erodible bed was set to 40 ft, which is beyond the limits of degradation expected to occur over the next 50 years. A river-wide sub-surface investigation has not been performed to accurately locate bedrock in the active channel, but specific borings near bridges indicate 40 to 100 ft of sand in Kansas City.

### Bed Sediment Gradation

Bed sediments were sampled at 5-mile increments in 1994 over the entire model reach. The model bed sediment was a weighted average of 50% of the individual sediment sample and 50% of the reach-average sediment sample. The average reaches were defined as follows: RM 500 to 391 (Rulo to Platte River), RM 391 to 250 (Platte River to Grand River), RM 250 to 130 (Grand River to Osage River), and RM 130 to 0 (Osage River to the mouth). Table 3 presents the original, 1994 data (interpolated to standard sizes) compared to the model bed gradations.

Table 3. Initial and Final Model Gradations, Percent Finer (Rounded to Whole Numbers)

RM	Original Data									Model Data								
	Diameter (mm)									Diameter (mm)								
	0.125	0.25	0.5	1	2	4	8	16	32	0.125	0.25	0.5	1	2	4	8	16	32
1	1	12	49	77	89	94	98	100	100	1	12	49	77	89	94	98	100	100
5	0	25	59	79	90	96	99	100	100	0	25	58	79	90	96	99	100	100
10	1	9	46	76	90	97	99	100	100	1	10	46	76	90	96	99	100	100
15	1	9	38	71	88	95	98	100	100	1	9	39	71	88	95	98	100	100
20	1	22	57	78	90	96	99	100	100	1	22	56	78	90	96	99	100	100
25	2	31	74	84	91	96	99	100	100	2	30	72	84	91	96	99	100	100
30	1	20	61	83	94	98	99	100	100	1	20	61	83	93	98	99	100	100
35	1	24	54	74	89	97	99	100	100	1	23	54	74	89	97	99	100	100
40	0	9	37	62	82	94	98	100	100	0	9	37	63	82	94	98	100	100
45	1	10	35	60	80	93	98	100	100	1	10	36	61	81	93	98	100	100

RM	Original Data									Model Data								
	Diameter (mm)									Diameter (mm)								
	0.125	0.25	0.5	1	2	4	8	16	32	0.125	0.25	0.5	1	2	4	8	16	32
50	0	8	39	72	90	97	99	100	100	0	8	40	72	90	97	99	100	100
55	1	9	36	63	80	91	97	100	100	1	9	37	63	81	92	97	100	100
60	0	17	55	74	89	97	99	100	100	0	17	54	74	89	97	99	100	100
65	1	23	53	75	89	94	96	99	100	1	23	53	75	88	94	97	99	100
70	0	8	36	65	84	93	97	99	100	0	9	36	65	84	93	97	100	100
75	1	12	40	61	75	86	95	99	100	1	12	40	61	76	87	95	99	100
80	1	15	42	71	87	92	96	98	100	1	15	42	71	87	93	96	98	100
85	1	18	52	77	92	98	100	100	100	1	17	52	77	91	98	100	100	100
90	1	14	49	66	81	92	98	100	100	1	14	49	66	81	92	98	100	100
95	1	9	44	72	89	97	100	100	100	1	9	44	72	89	97	100	100	100
100	1	14	45	79	94	98	100	100	100	1	14	45	78	94	98	100	100	100
105	1	29	66	86	95	99	100	100	100	1	29	66	85	95	99	100	100	100
110	3	22	64	84	92	97	99	100	100	3	22	64	83	92	97	99	100	100
115	0	5	36	65	81	93	98	100	100	0	6	37	65	81	93	98	100	100
120	0	12	50	77	89	95	98	100	100	1	12	50	76	89	95	98	100	100
125	1	24	54	72	85	94	99	100	100	1	24	54	72	85	94	99	100	100
130	1	16	62	86	95	98	99	100	100	1	16	62	86	94	98	99	100	100
135	1	12	48	67	79	91	98	100	100	1	12	49	68	80	92	98	100	100
140	1	15	54	85	96	99	100	100	100	1	15	55	85	96	99	100	100	100
145	3	26	62	77	87	94	98	100	100	3	26	62	78	87	94	98	100	100
150	1	28	67	84	94	97	98	100	100	1	28	67	84	94	97	98	100	100
155	6	47	70	82	92	98	100	100	100	5	46	70	83	93	98	100	100	100
160	1	31	74	85	91	95	98	100	100	1	30	73	85	91	95	98	100	100
165	2	31	70	86	93	97	99	100	100	2	31	69	86	93	97	99	100	100
170	1	9	62	88	96	99	100	100	100	1	10	62	88	96	99	100	100	100
175	1	12	54	79	91	97	99	100	100	1	13	55	79	91	97	99	100	100
180	1	23	74	91	97	99	100	100	100	1	23	73	91	97	99	100	100	100
185	2	27	62	91	99	100	100	100	100	2	27	62	91	99	100	100	100	100
190	1	24	66	85	93	98	100	100	100	1	24	66	85	93	98	100	100	100
195	1	14	51	75	88	95	99	100	100	1	15	52	76	89	96	99	100	100
196.6	0	13	43	76	92	97	99	100	100	0	14	44	76	92	97	99	100	100
200	1	25	67	85	95	99	100	100	100	1	25	67	85	95	99	100	100	100
205	0	14	55	81	93	97	99	100	100	0	15	55	81	93	97	99	100	100
210	1	15	61	85	96	99	100	100	100	1	16	62	85	96	99	100	100	100
215	2	35	75	93	99	100	100	100	100	2	34	74	93	98	100	100	100	100
220	1	17	70	93	98	99	100	100	100	1	17	70	93	98	99	100	100	100
225	1	25	69	93	99	99	99	100	100	1	25	69	93	98	99	99	100	100
230	2	36	75	90	97	99	100	100	100	2	35	74	90	96	99	100	100	100
235	1	33	76	95	100	100	100	100	100	1	33	76	95	99	100	100	100	100
240	1	28	59	76	89	96	99	100	100	1	28	59	76	89	97	99	100	100
245	1	29	72	87	94	98	99	100	100	1	29	72	87	94	98	99	100	100
250	1	22	70	92	98	99	100	100	100	1	22	70	91	97	99	100	100	100
255	1	35	80	96	99	100	100	100	100	1	34	79	95	99	100	100	100	100
260	1	29	71	88	94	97	99	100	100	1	29	71	88	94	97	99	100	100

RM	Original Data									Model Data								
	Diameter (mm)									Diameter (mm)								
	0.125	0.25	0.5	1	2	4	8	16	32	0.125	0.25	0.5	1	2	4	8	16	32
265	2	39	83	95	98	100	100	100	100	2	38	83	94	98	99	100	100	100
270	1	37	87	96	98	98	99	100	100	1	36	86	95	98	98	99	100	100
275	2	38	69	85	93	97	98	100	100	2	37	69	85	93	97	98	100	100
280	2	47	85	97	99	100	100	100	100	2	46	85	97	99	100	100	100	100
285	1	30	80	95	98	99	100	100	100	1	30	79	94	98	99	100	100	100
290	1	28	62	81	95	99	100	100	100	1	28	62	82	95	99	100	100	100
295	1	25	69	90	98	100	100	100	100	1	25	69	90	98	100	100	100	100
300	1	19	59	83	94	98	99	100	100	1	19	60	84	94	98	99	100	100
305	1	21	52	76	91	97	99	100	100	1	21	53	77	92	97	99	100	100
310	1	36	78	95	99	100	100	100	100	1	36	77	95	99	100	100	100	100
315	9	28	76	92	97	99	100	100	100	8	28	76	92	97	99	100	100	100
320	1	12	57	83	91	93	95	95	99	1	12	58	83	91	94	95	95	100
325	1	19	68	91	97	99	100	100	100	1	19	68	91	97	99	100	100	100
330	1	20	49	79	93	97	98	100	100	1	20	50	79	93	97	98	100	100
335	1	20	53	76	90	97	100	100	100	1	20	53	77	90	97	100	100	100
340	2	27	81	96	99	100	100	100	100	2	27	81	95	99	100	100	100	100
345	1	13	63	89	96	98	99	100	100	1	13	63	89	96	98	99	100	100
355	2	36	71	89	94	96	98	100	100	2	36	71	89	95	96	98	100	100
360	1	39	82	93	97	99	100	100	100	1	38	81	93	97	99	100	100	100
365	2	26	53	75	89	96	99	100	100	2	26	54	76	90	96	99	100	100
370	0	17	68	89	96	98	99	100	100	1	17	68	89	96	98	99	100	100
375	1	36	78	95	99	100	100	100	100	1	35	78	95	99	100	100	100	100
380	1	21	60	82	93	98	99	100	100	1	22	60	82	93	98	99	100	100
385	1	22	68	89	95	97	99	100	100	1	22	68	89	95	97	99	100	100
390	1	28	86	98	99	99	99	100	100	1	28	85	97	99	99	99	100	100
395	1	32	74	83	89	95	98	99	100	1	32	74	84	90	95	98	99	100
400	1	42	84	95	98	99	99	100	100	1	41	83	94	98	99	100	100	100
405	0	20	72	94	99	99	100	100	100	0	20	72	94	98	99	100	100	100
410	1	31	85	94	98	99	100	100	100	1	31	85	94	98	99	100	100	100
415	3	45	89	98	100	100	100	100	100	3	44	88	98	100	100	100	100	100
420	1	18	70	92	97	99	100	100	100	1	18	70	92	97	99	100	100	100
425	1	36	80	93	98	99	100	100	100	1	36	79	93	98	99	100	100	100
430	2	37	82	94	98	99	100	100	100	2	36	82	94	98	99	100	100	100
435	1	23	80	97	100	100	100	100	100	1	24	80	97	99	100	100	100	100
440	0	14	66	89	95	97	99	100	100	0	15	67	89	95	97	99	100	100
450	1	26	80	94	98	99	100	100	100	1	26	79	94	98	99	100	100	100
460	0	29	72	89	96	99	100	100	100	1	29	72	89	97	99	100	100	100
465	1	15	61	80	91	97	99	100	100	1	16	62	80	91	97	99	100	100
470	1	33	75	91	97	99	100	100	100	1	33	75	91	97	99	100	100	100
475	1	24	77	96	99	100	100	100	100	1	25	77	96	99	100	100	100	100
480	0	21	72	94	99	100	100	100	100	0	21	72	94	99	100	100	100	100
485	1	29	77	96	99	100	100	100	100	1	28	77	95	99	100	100	100	100
490	1	14	57	87	96	98	100	100	100	1	15	58	88	96	98	100	100	100
495	1	17	50	80	93	98	99	100	100	1	18	51	81	93	98	99	100	100

### 3.4 Boundary Conditions

Boundary conditions include flow, water temperature, downstream water surface elevation, incoming sediment load and gradation, floodplain deposition amounts, and dredging amounts, locations, and timing. These boundary conditions are described in the following paragraphs.

#### Flows

Daily flow values from Aug 1, 1994 – 29 July 2014, computed from seven mainstem Missouri River and seven tributary USGS gaging stations, were used as the flow inputs to the model.

Daily flow values were compiled for the following USGS gage stations listed in Table 4. The model upstream boundary was set to the daily flow reported by USGS for the Missouri River at Rulo, Nebraska. Each tributary was entered as a lateral flow. The difference between the mainstem Missouri River gages that could not be explained by the tributary flows were entered as uniform lateral flows. These uniform lateral flows account for ungaged inflows, totaling 19% of the total flow volume at St. Charles, MO. They also approximate the longitudinal change in the flow profile due to timing effects which are not modeled in quasi-unsteady flow modeling. This same approximation was utilized in USACE (2017a). Additional details regarding drainage area delineations for the watershed are included in the Unsteady HEC-RAS Model Calibration Report, Appendix E.

Scaled down versions (1/10,000) of these uniform lateral flows were entered in order to trigger the floodplain deposition rating curves at the appropriate times. The scaled-down uniform flows are very small and have negligible effect on actual model flows.

The flows from the downstream gage are used in the model as lateral flows and as input to the rating curves. At two gages, insufficient sediment data exists at the downstream gage, so the flow/load relationship was developed from a more upstream gage. These relationships were then used with flows from the downstream gages.

Table 4. USGS Gage Stations Used in the Model

USGS Gage #	Name	USGS Drainage Area (sq mi)
06813500	Missouri River at Rulo, NE	414,900
06818000	Missouri River at St. Joseph, MO	426,500
06893000	Missouri River at Kansas City, MO	484,100
06895500	Missouri River at Waverly, MO	485,900
06909000	Missouri River at Boonville, MO	500,700
06934500	Missouri River at Hermann, MO	522,500
06935965	Missouri River at St. Charles, MO	542,000
06817700	Nodaway River Near Graham, MO	1,520
06817000	Nodaway River at Clarinda, IA*	762

USGS Gage #	Name	USGS Drainage Area (sq mi)
06821190	Platte River at Sharps Station, MO	2,380
06892350	Kansas River at Desoto, KS	59,756
06902000	Grand River Near Sumner, MO	6,880
06905500	Chariton River Near Praire Hill, MO	1,870
06926510	Osage River below St. Thomas, MO	14,584
06934000	Gasconade River Near Rich Fountain, MO	3,180
06933500	Gasconade River Near Jerome, MO*	2,840

\* Denotes a gage used for development of the flow/sediment rating curve but not used as the flow input.

### **Water Temperature**

The HEC-RAS sediment model requires a water temperature for each day of the simulation to calculate fall velocity. The annual time series of water temperatures based on measurements at the Kansas City gage, as developed in USACE (2017a), was used in this model.

### **Downstream Water Surface Boundary Condition**

The downstream water surface elevation was originally set to the water surface elevation computed by the Missouri River Recovery Program (MRRP) unsteady flow model which includes the backwater effect from the Mississippi River. However, on inspection, the model water surface output at this location would occasionally drop below the normal depth solution, which produced unreasonably high velocities and excessive scour. To decrease this unrealistic effect, a floor of 1 ft below the normal depth solution (computed from the initial geometry) was imposed. This maintains the backwater effects from the Mississippi River included in the MRRP unsteady flow model. Figure 18 indicates the downstream boundary as a function of the flow in the MRRP unsteady flow model at RS 0.73.

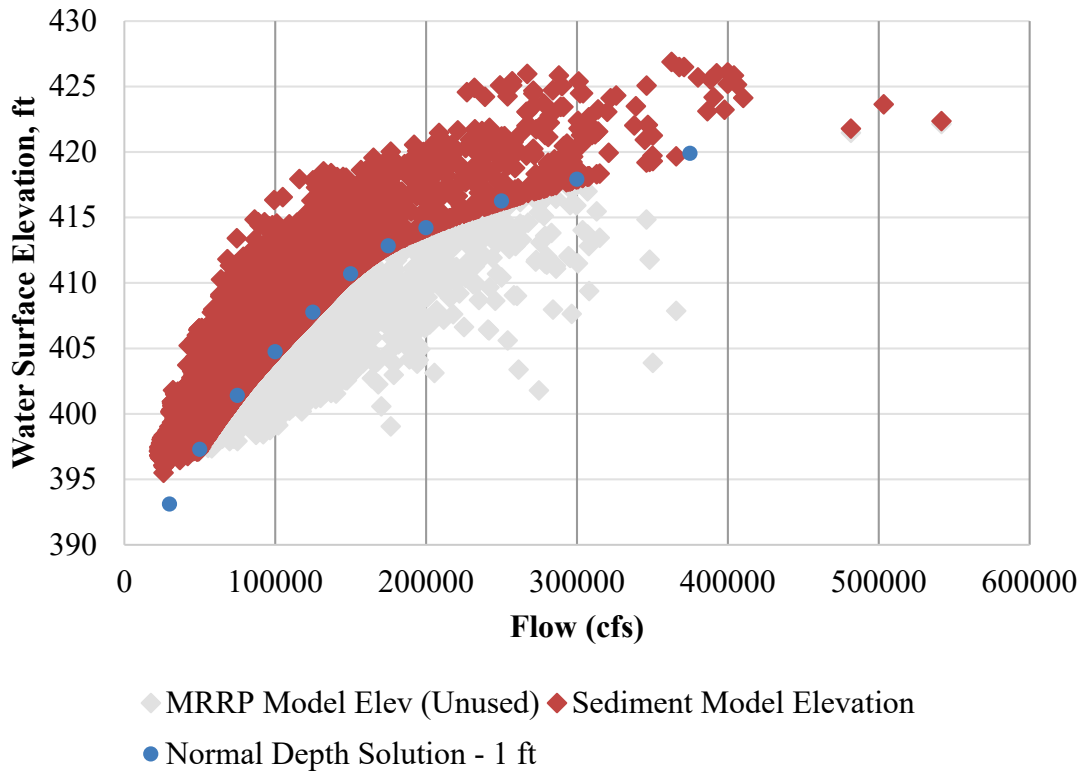


Figure 18. Downstream Boundary Condition

**Sediment Load**

The incoming sediment load and gradation was computed and entered into the model as a DSS time series for each grain class. The sediment load for a given grain class was computed as the total suspended sediment load multiplied by the percent of the suspended load corresponding to the grain class plus the total bed load multiplied by the percent of the bed load corresponding to that grain class.

Only sands and gravels were included in the model. Finer sediments are wash load in this system; they are not found in appreciable quantities on the bed and do not play a significant role in the physical bed change processes. Wash load causes a numerical artifact in HEC-RAS 5.0.3 and so was not included.

USGS Water Quality data at Saint Joseph, MO were used to develop the flow/load relationship and gradational breakdown of the suspended load. Overall, the suspended sediment load fines considerably with increasing discharge. Figure 17 demonstrates the average, calibrated total load relationships at Saint Joseph compared to USGS measurements for suspended load. (Note that the USGS report many suspended sediment samples that had no coarse sand, which could not be

plotted in log space on Figure 19.) These loads computed for St. Joseph were reduced by the Nodaway sediment load in order to create the model upstream boundary condition.

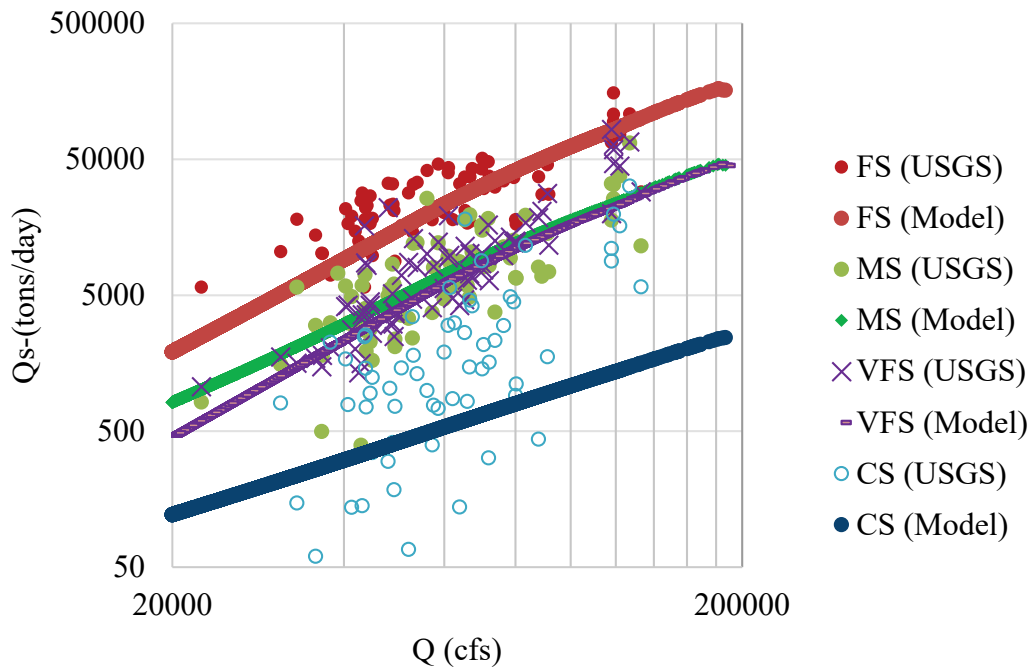


Figure 19. Average relationships at Saint Joseph used to develop upstream rating curve vs. measured suspended sand by grain class

During the 2011 flood, the high volumes of relatively clear water released from the dams resulted in a markedly different suspended sediment relationship. The suspended loads during the 2011 event was based on USGS measurements during the event rather than the long-term relationship shown above.

The bedload portion of the sediment load was computed from the bedload rating curve for St. Joseph presented in Abraham et al. (2017). This bedload rating curve was computed by using successive multi-beam bathymetric surveys (Abraham et al. 2011) with the time correction suggested in Shelley et al. (2013). This rating curve is provided in Figure 20.

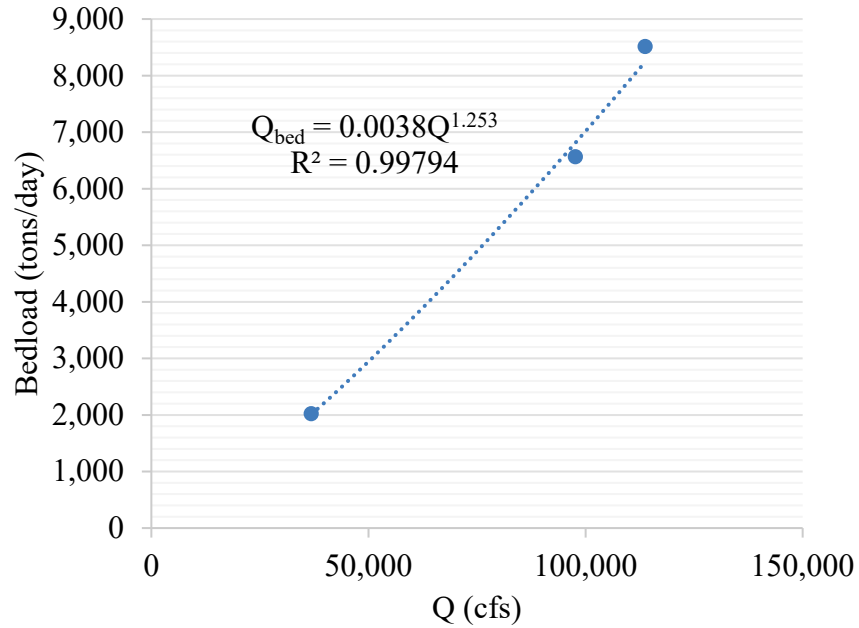


Figure 20. Missouri River Bedload Rating Curve at St. Joseph (from Abraham et al. 2017)

The gradation of the incoming total sediment load is a function of the relative contributions from bed load and suspended load, which varies by flow and by whether the 1994 – 2010 or 2011 flow-load curve is used for the suspended sediment contribution.

Sediment rating curves at seven major tributaries were included in the model as flow-load boundary conditions. This report presents the calculated rating curves—the model itself includes these rating curves with the loads divided by two to compensate for a RAS 5.0.3 bug that doubles tributary loads.

The flow-load curve for the Nodaway River was based on USGS gage data for the Nodaway River at Clarinda, MO. USGS data yielded the gradational breakout of the suspended fines and sands, with over 93% of the suspended sediment load composed of silts and clays. Bed load data was assumed to be 1% of suspended with predominantly fine and medium sand. Table 5 and Figure 21 provide the rating curve for the Nodaway River.

Table 5. Nodaway River Model Bed Material Rating Curve

Q (cfs)	100	2,000	10,000	150,000
Qs (tons/day)	2	1,333	31,200	67,002
VFS	1	436	10,200	21,905
FS	1	556	13,200	28,347
MS	0	205	4,800	10,308
CS	0	77	1,600	3,436
VCS	0	60	1,400	3,007

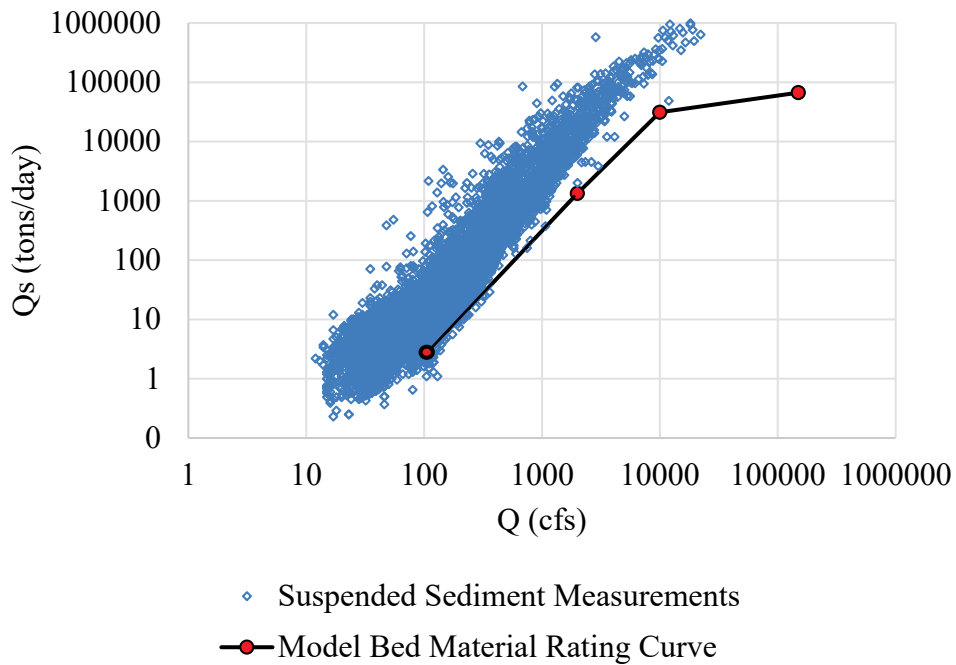


Figure 21. Nodaway River Sediment Loads

The flow-load curve for the Platte River was based on USGS gage data for the Platte River at Sharps Station. A bed material load was developed by subtracting the percent fines recorded in USGS measurements (which increases with increasing flow) and adding 5% as an estimate for bed load. In the absence of measurements, the bed load was assumed composed of very fine, fine, and medium sand. Table 6 and Figure 22 provide the loads and gradations used in the model.

Table 6. Platte River Bed Material Load Rating Curve and Gradation

Q (cfs)	1	1000	5000	10000	50000
Qs (tons/day)	0.004	426	5337	8454	10305
VFS	0.002	265	3149	4763	5504
FS	0.001	151	2004	3322	4247
MS	0.0000	10	184	369	554

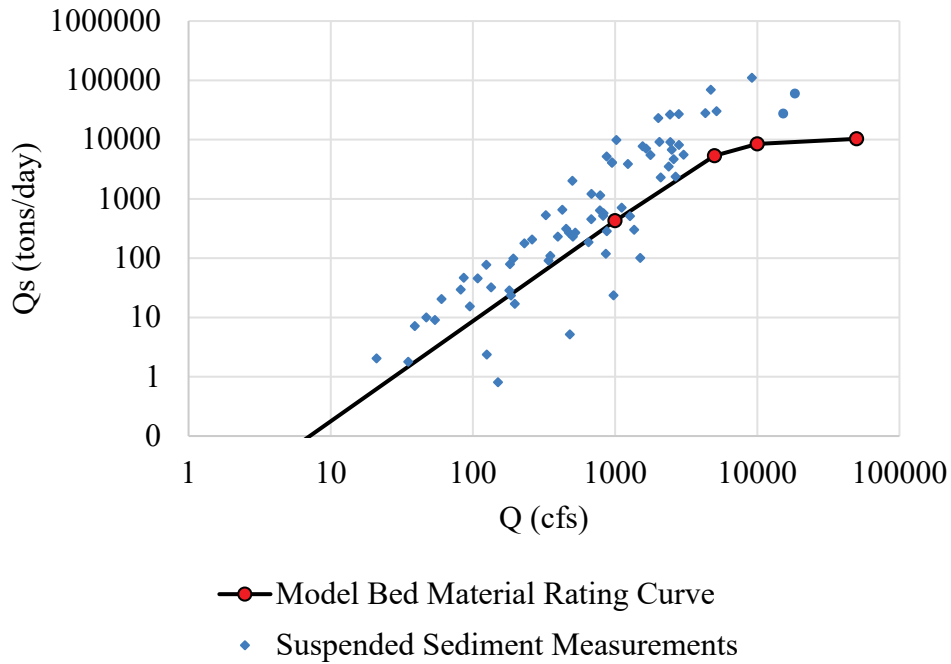


Figure 22. Platte River Sediment Loads

The sediment load and gradation for the Kansas River was based on USGS gage data for the Kansas River at Desoto, Kansas. Bed load data was assumed to be 5% of suspended with predominantly fine, medium, and coarse sand. The Kansas River experiences multiple anthropogenic influences on the sediment load in between the sediment gaging station and the confluence with the Missouri River, including multiple channel mining operations and multiple weirs. Table 7 and Figure 23 provide the rating curve for the Kansas River.

Table 7. Kansas River Bed Material Load Rating Curve and Gradation

Q (cfs)	250	6000	40000	100000	150000
Q <sub>s</sub> (tons/day)	4	1544	51736	240000	404168
VFS	0.4	160	5278	53418	53418
FS	0.8	568	25922	337534	337534
MS	2.4	738	18236	163036	163036
CS	0	56	1532	20120	20120
VCS	0	20	768	10060	10060

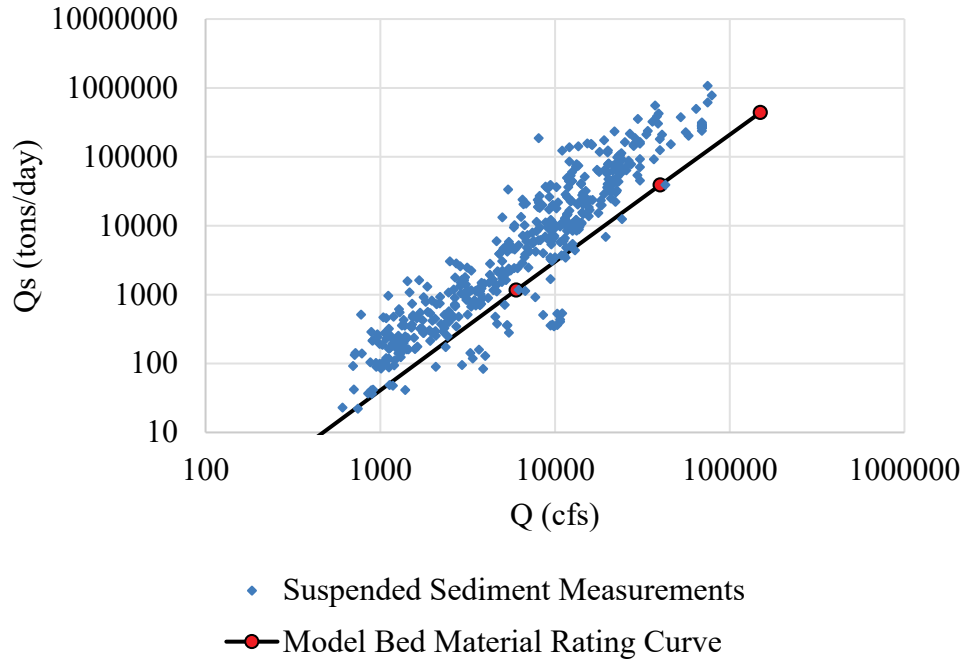


Figure 23. Kansas River Sediment Loads

The sediment load and gradation for the Grand River was based on USGS gage data for the Grand River at Sumner, Missouri. USGS data yielded overall concentrations and % fines. The gradational breakout of the suspended sands was assumed to be predominantly very fine and fine sand. Bed load data was assumed to be 5% of suspended with predominantly fine and medium sand. Table 8 and Figure 24 provide the rating curve for the Grand River.

Table 8. Grand River Bed Material Load Rating Curve and Gradation

Q (cfs)	100	1000	33000	100000
Qs (tons/day)	9	337	61540	70028
VFS	3	128	19361	21181
FS	4	139	25258	28701
MS	2	74	14648	16914
CS	0	10	4279	5387

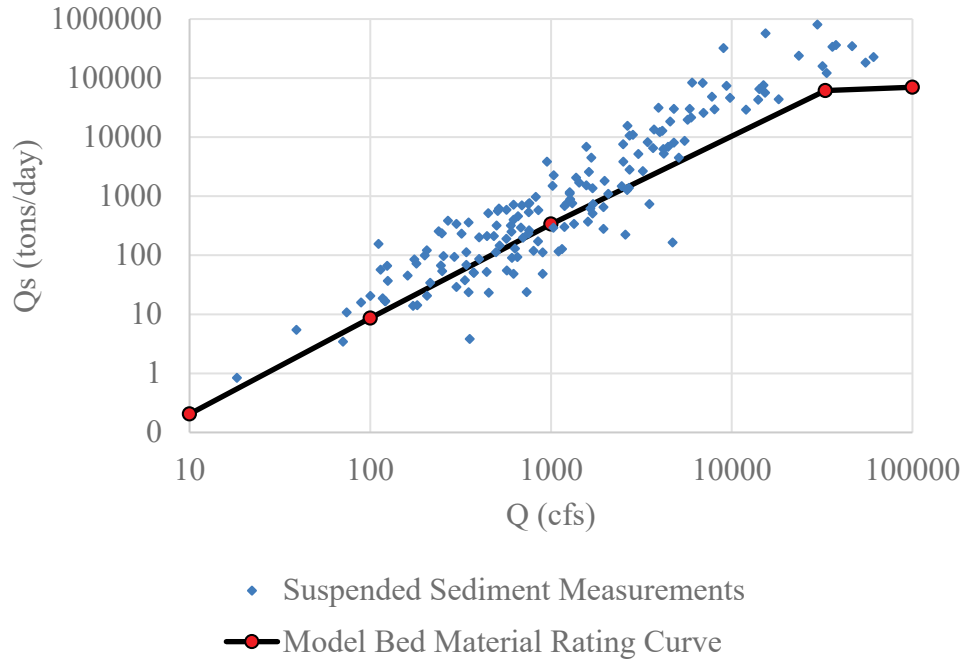


Figure 24. Grand River Sediment Loads

The sediment load and gradation for the Chariton River was based on USGS gage data for the Chariton River near Prairie Hill, MO. USGS data yielded the gradational breakout of the suspended fines and sands. Bed load data was assumed to be 5% of suspended with predominantly fine and medium sand. Table 9 and Figure 25 provide the rating curve for the Chariton River.

Table 9. Chariton River Bed Material Load Rating Curve and Gradation

Q (cfs)	20	10000	150000
Qs (tons/day)	0.1	3927	22305
VFS	0.00	222	1188
FS	0.05	2536	14505
MS	0.01	588	3311
CS	0.01	390	2201
VCS	0.00	191	1100

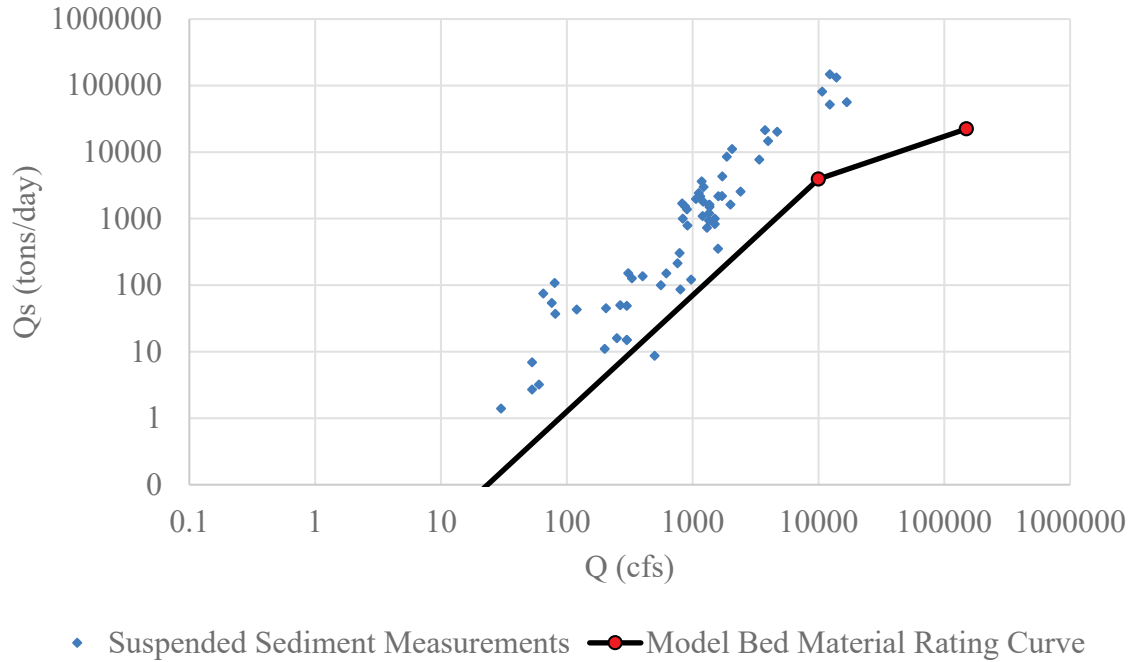


Figure 25. Chariton River Sediment Loads

The sediment load and gradation for the Osage River was based on USGS gage data for the Osage River below St. Thomas, MO. USGS data yielded overall concentrations and % fines. The gradational breakout of the suspended sands was assumed to be predominantly fine and medium sand. Bed load data was assumed to be 5% of suspended with predominantly fine and medium sand. Table 10 and Figure 26 provide the rating curve for the Osage River.

Table 10. Osage River Bed Material Load Rating Curve and Gradation

Q (cfs)	100	1000	5000	40000	100000
Qs (tons/day)	6	66	350	2993	4581
VFS	0.5	6	31	257	388
FS	1.7	19	101	856	1304
MS	2.9	33	175	1497	2291
CS	0.6	7	39	342	528
VCS	0.1	1	4	42	70

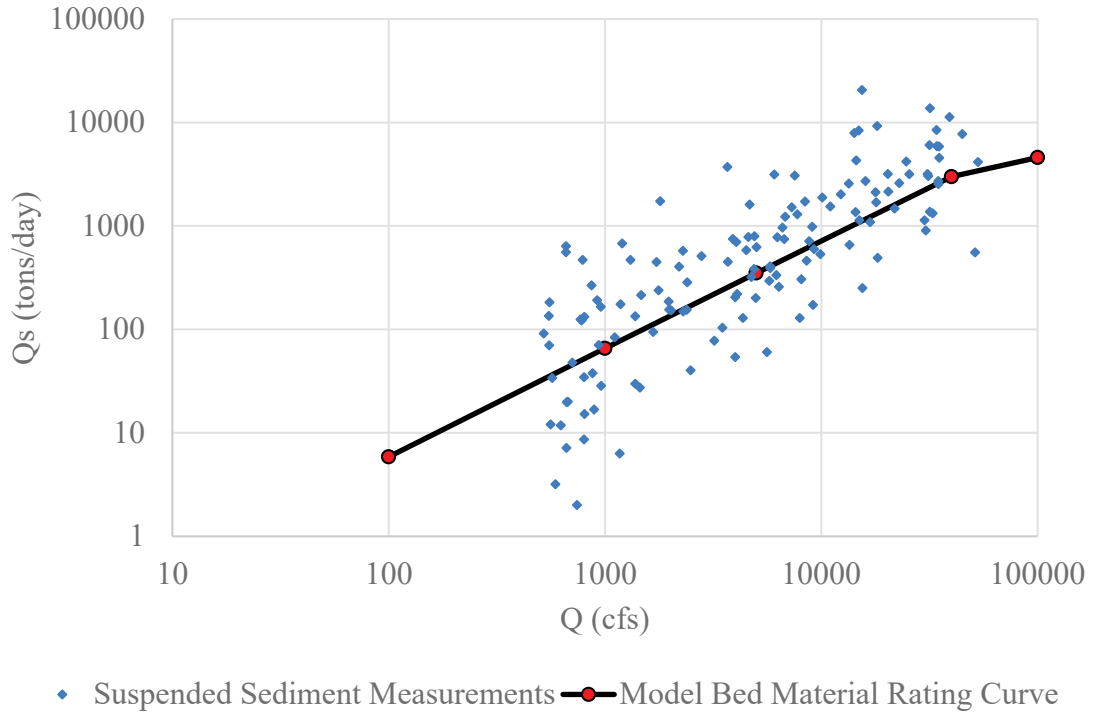


Figure 26. Osage River Sediment Loads

The sediment load and gradation for the Gasconade River was based on USGS gage data for the Gasconade River at Jerome, MO. USGS data yielded overall concentrations. The % fines was taken from the Osage River and the same assumptions were made for the gradational breakout of sands and bed load as the Osage River.

Table 11. Gasconade River Bed Material Load Rating Curve

Q (cfs)	100	1000	5000	25000	100000
Qs (tons/day)	1	59	1085	19839	95736
VFS	0.1	5	95	1714	8109
FS	0.3	17	312	5681	27256
MS	0.4	29	542	9919	47868
CS	0.1	6	122	2254	11038
VCS	0.0	1	13	270	1465

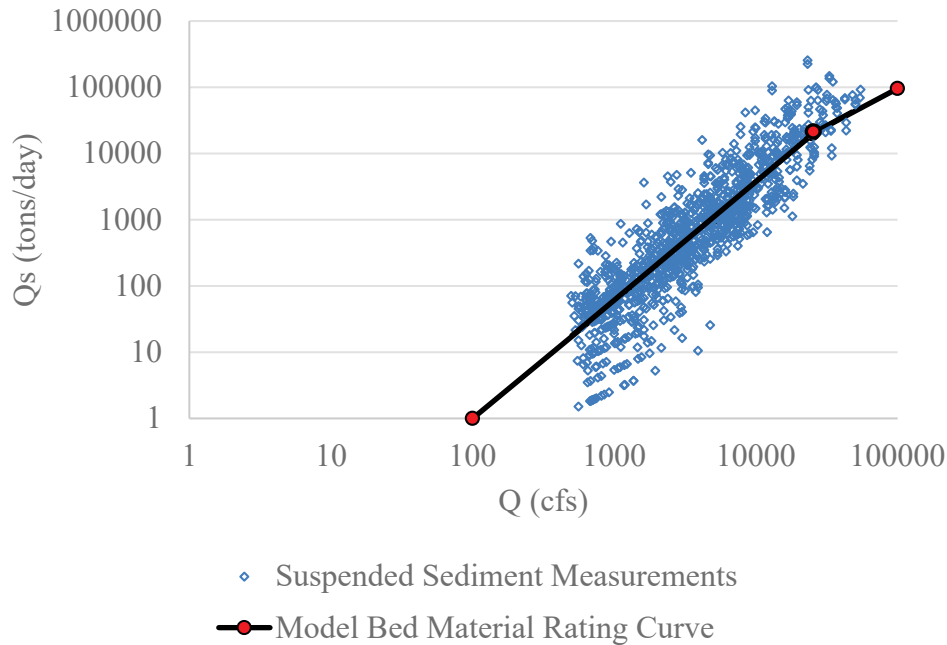


Figure 27. Gasconade River Sediment Loads

### 2011 Flood Boundary Conditions

As shown in Figure 3, the sediment concentrations were dramatically lower during the 2011 flood than typical. For March – November, 2011, the suspended sediment load was computed by the formula  $Q_s = 0.7641 Q + 6910.7$ , where  $Q_s$  = suspended sediment in tons/day and  $Q$  = daily flow in cfs. Bedload, computed with the rating curve depicted in Figure 20, was added to this value to yield the total bed material load for the day at St. Joseph. This load was transferred upstream by subtracting the load for the Nodaway. This flow/load/gradation curve is unique to the 2011 event.

### Dredging

Commercial dredging on the Missouri River was a significant driver of bed degradation during the calibration period (USACE 2011). The resolution of dredging data varies over time. From 1994 – 1996, the annual tons dredged were reported to USACE’s regulatory branch on a reach basis. Since 1997, daily tons dredged and river miles were reported.

Dredging was included in the degradation model as monthly totals at each cross-section with the start date the first day of the month and the end date the last day of the month. For 1997 and later, the reported monthly tonnages of dredging were assigned to the appropriate cross-sections and to the appropriate month. Annual, reach-scale tonnages for 1994 – 1996, were apportioned according to the temporal and spatial distribution of dredging from 1997 – 2009. Figure 28 provides the spatial distribution for dredging for each year.

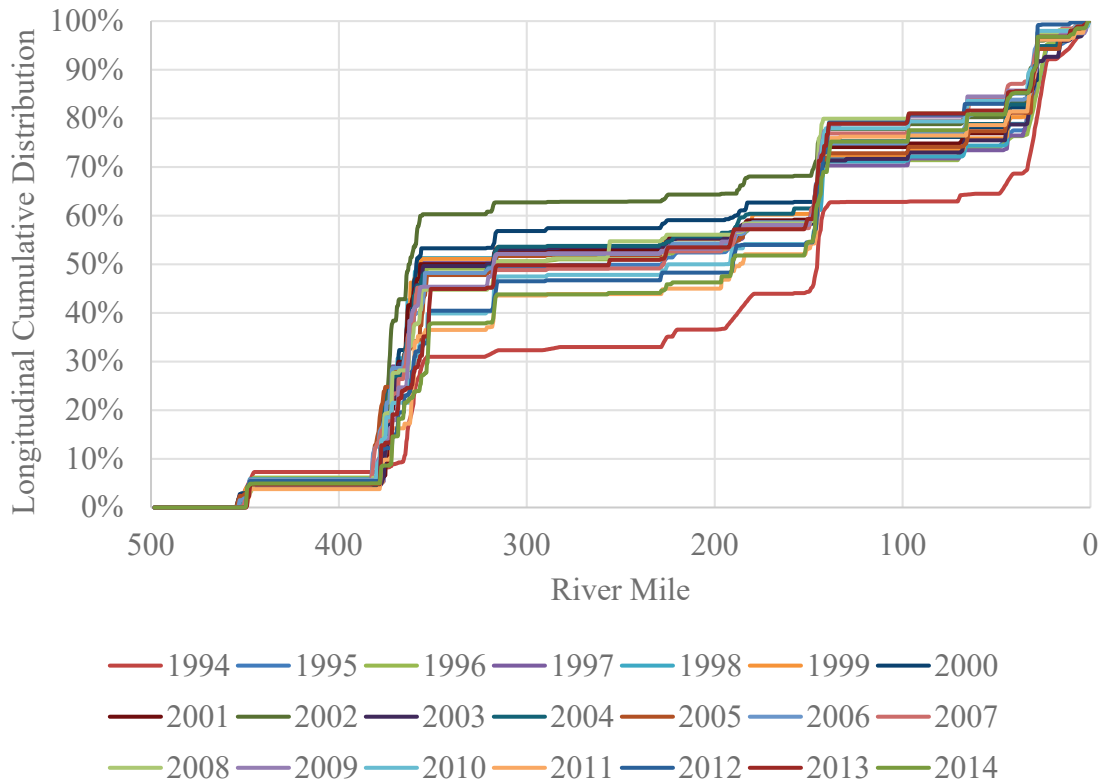


Figure 28. Longitudinal Cumulative Dredging Distribution by River Mile

The impact of dredging was restricted to the actual dredging tonnage, i.e. one ton of extracted material lowers the bed by a volume equivalent to one ton. Potential dredging effects due to material sorting, re-discharge, and bed disturbance were not included. Dredging volumes or locations were not adjusted during calibration.

**Unmeasured Sediment Inflows**

Sediment budgeting was used to estimate unmeasured sediment inflows for inclusion in the model. A sediment budget quantifies the terms in the continuity equation: Sediment\_In – Sediment\_Out= Δ Storage. The following equation provides the sediment budget from the St. Joseph to the Kansas City gages, from 1994 to 2005:

$$SJ + PR + KR + UnM - D - FP - KC = \Delta Bed \quad \text{(Equation 1)}$$

Where SJ = the sand load passing the Saint Joseph gage (tons)

PR = the sand input from the Platte River (tons)

KR = the sand input from the Kansas River (tons)

UnM = the unmeasured sediment inflows (tons)

D = the dredging volume (tons)

KC = the sand load passing the Kansas City gage (tons)

$\Delta$ Bed = the total mass of bed change (tons)

PR, KR, and KC were taken from USGS (Heimann et al. 2010), using model rating curves to fill in the gaps as needed. As a full 2005 bathymetric survey is not available, the 1994 – 2007 bed change was divided by 13 years then multiplied by 11 years to approximate the 1994 – 2005 bed change. Floodplain deposition (FP) was assumed negligible for 1994 to 2009. The unmeasured sediment (UnM) was solved for arithmetically. Table 12 presents the numerical values for each variable. (Note: Significant digits are retained to the ton in Tables 12 – 14 to make the math reproducible, not to imply that any of these quantities are known to the ton.)

Table 12. Sediment Budget 1994 – 2005 for St. Joseph to Kansas City

Budget Term	Mass (tons)
SJ	116,179,350
PR	3,345,417
KR	10,091,852
<b>UnM</b>	10,778,755
D	20,981,695
FP	0
KC	147,369,350
$\Delta$ Bed	-27,955,671

A similar analysis was performed for the reach from Kansas City, MO to Herman, MO. Table 13 presents the numerical values for each variable.

$$KC + GR + CH + OS + GS + UnM - D - FP - HR = \Delta Bed \quad (\text{Equation 2})$$

Where KC = the sand load passing the Kansas City gage (tons)

GR = the sand input from the Grand River (tons)

CH = the sand input from the Chariton River (tons)

OS = the sand input from the Osage River (tons)

GS = the sand input from the Gasconade River (tons)

UnM = the unmeasured sediment inflows (tons)

D = the dredging volume (tons)

HR = the sand load passing the Hermann gage (tons)

$\Delta$ Bed = the total mass of bed change (tons)

Table 13. Sediment Budget 1994 – 2005 for Kansas City to Hermann

Budget Term	Mass (tons)
KC	147,369,350
GR	13,796,832
CH	492,949
OS	2,792,519
GS	3,136,888
<b>UnM</b>	60,718,243
D	36,042,315
FP	0
HR	199,524,347
$\Delta$ Bed	-7,259,881

The unmeasured sediment load incorporates all non-specific sediment sources needed for the sediment budget to balance, including bank erosion, gullies, tributaries, and shallow water habitat construction activities. In addition, the unmeasured term incorporates error in the upstream, downstream, and tributary rating curves. The procedure used to input this sediment to the model causes the needed additional sediment to be more or less uniformly distributed between the gages.

The UnM values listed in Tables 12 and 13 were entered into the model using rating curves tied to the flow boundary conditions representing ungaged inflows. Rating curves of the type  $Q_s = aQ$ , were created, with  $a$  set so that the sum of  $Q_s$  from 1994 to 2005 equals the UnM values presented in Tables 12 and 13.

The flows that drive the unmeasured sediment rating curves are scaled-down versions of the ungaged water inflows. These inflows were computed as the difference between flows at gages that are not accounted for by tributary inflows. On any given day, differences in flows at gages may be negative due to unsteady hydrograph effects. To avoid problems with the rating curves during negative uniform lateral flows, separate flow boundary conditions that are always positive were created for use with the unmeasured sediment rating curves. These separate flow boundary conditions were scaled down by 10,000 so that only negligible additional flow is added.

**Floodplain Deposition**

As depicted in Figure 2, levees which line most of the Missouri River confine flows to a narrow corridor. These levees reduce floodplain deposition of sediments during moderately high flows, but very high flows which overtop levees can deposit tremendous volumes of sediment on the

floodplain. While the precise volumes of floodplain deposition cannot be quantified with existing data, available data do allow approximations based on sediment budgeting (1993 flood) and aerial photographic analysis (2011 flood).

**1993 Flood**

A sediment budget analysis similar to that presented in the previous section was performed from 1987 to 1994. This time period includes the historic flood of 1993 which deposited tremendous quantities of sediment on the floodplain. The Soil Conservation Service (SCS 1993) reports that the 1993 flood deposited 546 million cubic yards of sediment on the floodplain, though this value includes sediments sourced from significant scour holes in the floodplain as well as the from the channel. Sediment budget analyses Equations 1 and 2 were used to determine the floodplain deposition amount (FP) to be sourced from the channel during the 1993 flood. The unged sediment contribution was computed using the *a* and *b* values computed from the analysis described in the previous section. Tables 14 and 15 provide the computed values.

Table 14. Sediment Budget 1987 – 1994 for St. Joseph to Kansas City. Used to solve for the 1993 floodplain deposition.

Budget Term	Mass (tons)
SJ	72,440,000
PR	1,647,389
KR	13,151,706
UnG	8,978,963
D	1,600,786
<b>FP</b>	<b>51,071,910</b>
KC	84,240,000
ΔBed	-40,694,638

Table 15. Sediment Budget 1987 – 1994 for Kansas City to Hermann. Used to solve for the 1993 floodplain deposition.

Budget Term	Mass (tons)
KC	84,240,000
GR	7,039,551
CH	234,738
OS	1,475,300
GS	1,678,128
UnG	14,977,292
D	20,980,378
<b>FP</b>	<b>98,220,908</b>

HR	84,240,000
$\Delta\text{Bed}$	-152,526,276

This analysis computes 149 million tons of channel sediments deposited on the floodplain during the 1993 flood from St. Joseph, MO to Hermann, MO. Extending the analysis to the entire model space with the same overall tons/mile rate of deposition = 212,422,000 total tons of floodplain deposition during the 1993 flood.

**2011 Flood**

The floodplain deposition amount for the 2011 flood was computing following the same analysis used in USACE (2017), which is the aerial extend of sand deposition from Alexander et. al, (2013) times the suggested minimum depth of 2 ft. See Figure 29.

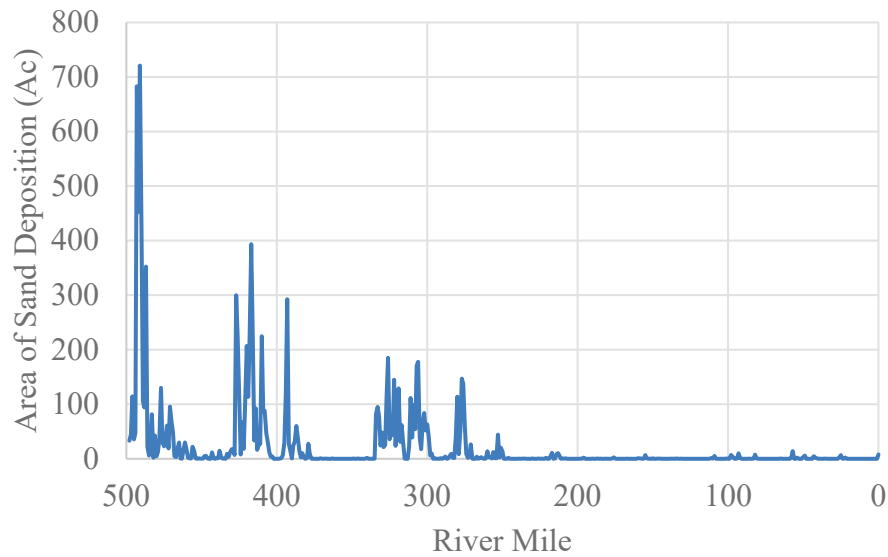


Figure 29. Acreage of Floodplain Sand Deposition from the 2011 flood. Data from Alexander et. al (2013).

The 1993 and 2011 flood events offer two data points from which to interpolate and extrapolate floodplain deposition to other floodplain deposition events. This was accomplished by creating rating curves of the type  $FP = aQ^b$ , where  $Q$  = the daily flow in the mainstem Missouri River and  $a$  and  $b$  were chosen such that the total floodplain deposition over the flood event was correct for both the 1993 and the 2011 floods. For flows below a threshold,  $FP$  was assumed zero. Table 16 provides the parameters.

Table 16. Parameters Used for Floodplain Deposition

<b>Floodplain Equation</b>	<b>Gage(s)</b>	<b>Flow Threshold (cfs)</b>	<b>a</b>	<b>b</b>
#1	Rulo	160,000	5.84E-08	2.43
#2	St. Joseph	200,000	3.65E-06	2.43
#3	St. Joseph + Platte River	200,000	3.65E-06	2.43
#4	Waverly	200,000	1.22	1.21
#5	Boonville	260,000	1.22	1.21
#6	Boonville	260,000	2.53	1.21

The sediment loads so calculated were entered into the model as lateral loads at discrete locations which correspond to the locations of the 2011 floodplain deposition. Several of the computed loads were split to two cross section locations to better distribute the effect of floodplain deposition. Table 17 indicates the lateral loads entered into the HEC-RAS model. In future projects, the same locations for floodplain deposition seen in the 2011 flood are used for any flood that exceeds the flow thresholds.

Table 17. Source of Lateral Loads for Floodplain Deposition

<b>RAS RS</b>	<b>Entered into RAS</b>
492.5	Eq#1 * 75%
478.4	Eq#1 * 25%
427.13	Eq#2
410.01	Eq#3
325.2	Eq#4 * 50%
301.97	Eq#4 * 25%
279.13	Eq#4 * 25%
187.55	Eq#5 * 50%
133.66	Eq#5 * 50%
88.92	Eq#6 * 50%
20.66	Eq#6 * 50%

Table 18 indicates that the model inputs closely match the best computed values for the 1993 and 2011 flood. Figure 30 presents the computed floodplain deposition and the location/magnitude entered into the model for the 2011 flood event. Values are negative because they draw sediment from the channel.

Table 18. Computed Floodplain Deposition vs. Included Model Floodplain Deposition

Reach	1993		2011	
	Computed (tons)	Model (tons)	Computed (tons)	Model (tons)
SJ to KC	-56,847,829	-56,751,019	-14,864,605	-14,832,221
KC to HR	-102,116,528	-101,748,539	-13,454,765	-13,406,075
Full Model	-225,539,173	-225,621,716	-45,695,231	-45,915,488

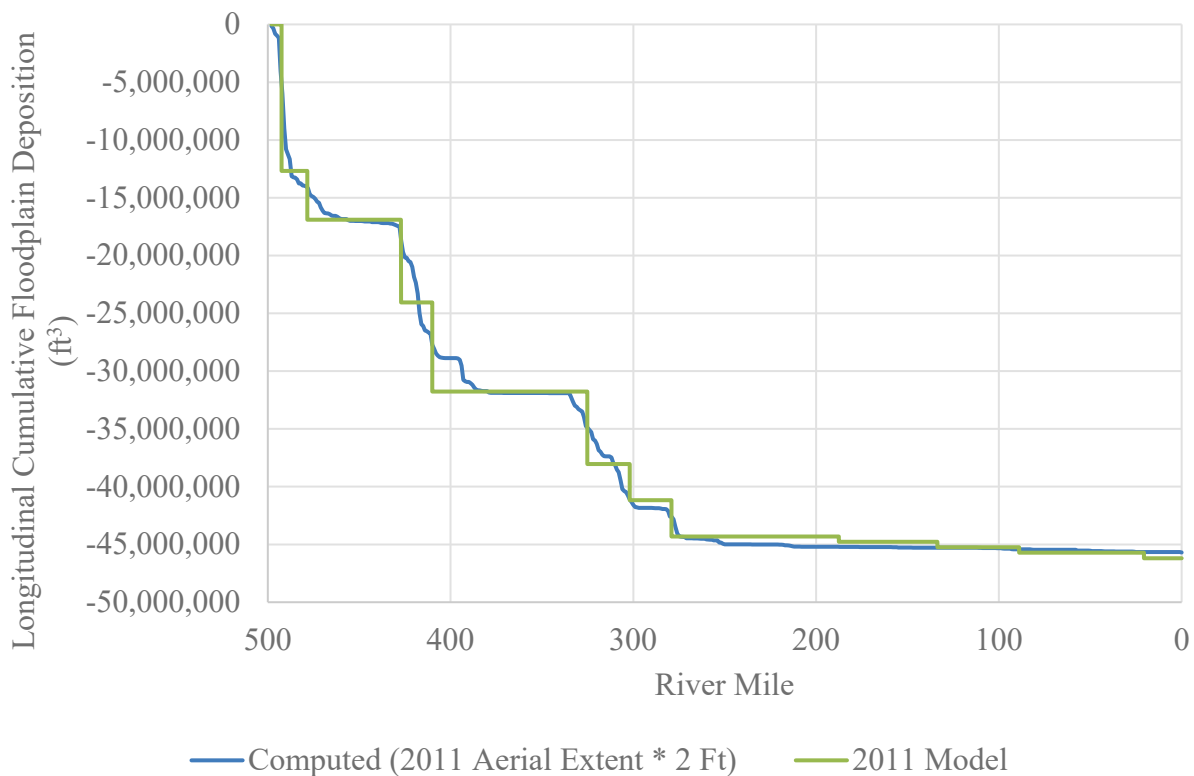


Figure 30. Floodplain Deposition in the Model During the 2011 Flood

### 3.5 Model Parameters

Model parameters include sediment transport formula, bed mixing algorithm, and computational time steps. These model parameters are described in the following paragraphs.

#### Sediment Transport Formula

Multiple sediment transport formula were tested, including Laursen-Copeland, Meyer-Peter and Muller, Toffaleti, and Yang. The Toffaleti (1968) sediment transport formula was selected to

compute the sediment transport capacity due to its applicability and history of use on large, sand-bed rivers including the Missouri River (USACE 2017) and because it yielded reasonable initial results. During calibration, it was found that Toffaleti produced insufficient transport during the flood of 2011. To increase the transport capacity at high flows, the combined Toffaleti/MPM function was used with a coefficient of 1 and a power of 1.5. This provides slightly more transport capacity, particularly at high flows. The Toffaleti fall velocity method was also used. HEC (2010) details the Toffaleti computational procedure.

### **Bed Mixing Algorithm**

Two bed mixing/armoring algorithms were tested: Exner 5 and Exner 7. Exner 7 produced excessive degradation compared to the prototype and was not selected. Exner 5 yielded reasonable results for total bed degradation and was selected for use in the model.

### **Computational Increment**

The computational increment was set based on the flow rate. It ranges from 24 hr when flow is less than 60,000 cfs to 30 min when flow exceeds 200,000 cfs. Bed exchange iterations per time step was set to 10, the HEC-RAS default.

## **4.0 Calibration/Verification**

The principle calibration period runs from Aug 1, 1994 to Oct 1, 2009. This time period includes a range of high and low flows and is most representative for future prediction. Water surface elevations at multiple gages, sediment loads, and repeat cross sections in 2007 and 2009 offer robust calibration data over this period. A second time period from Oct 1, 2009 to July 29, 2014 was also used in calibration. However, because this time period includes the historic Missouri River Flood of 2011 which exhibited unique boundary conditions, this time period serves more as a verification of reasonableness than a second calibration point. The principal parameters which were varied to achieve calibration were the Manning ‘n’ values for the active channel, inter-sill region, and inter-dike region, the flow-based ‘n’ adjustment factors, bed gradation data, the sediment loading from Kansas River and Grand River, and the moveable bed extents. As described in the previous paragraphs, these calibrated initial conditions and boundary conditions have physical basis in measured data.

### **Early Hydraulic Calibrations**

The model bathymetry is from 1994. The calibration period starts in Aug 1, 1994. On Aug 16 and 17, 1994, the water surface was measured at multiple points along the river. These measured water surface elevations are subject to greater error than USGS gage measurements but are still useful to verify the hydraulic model. Figures 31, 32, and 33 illustrate the model agreement to the low water surface elevations collected on August 16 and 17, 1994. The average absolute difference between modeled and measured water surfaces for August 16 and 17 is 0.8 ft. This analysis is similar to a “fixed-discharge, fixed-bed” analysis for a low discharge because it occurs so soon after the model start.

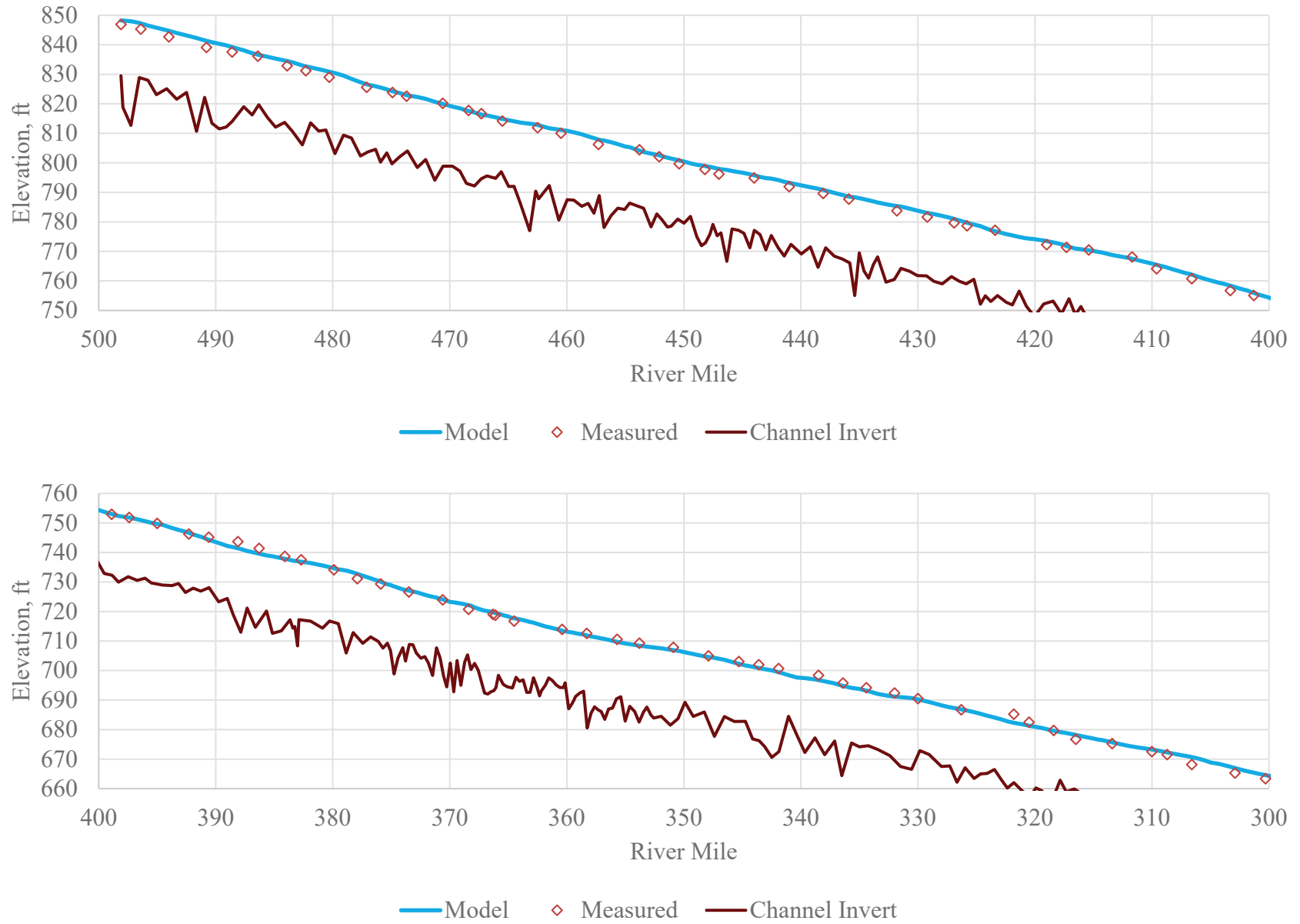


Figure 31. Model hydraulic comparison at low flow: River Miles 500 - 300

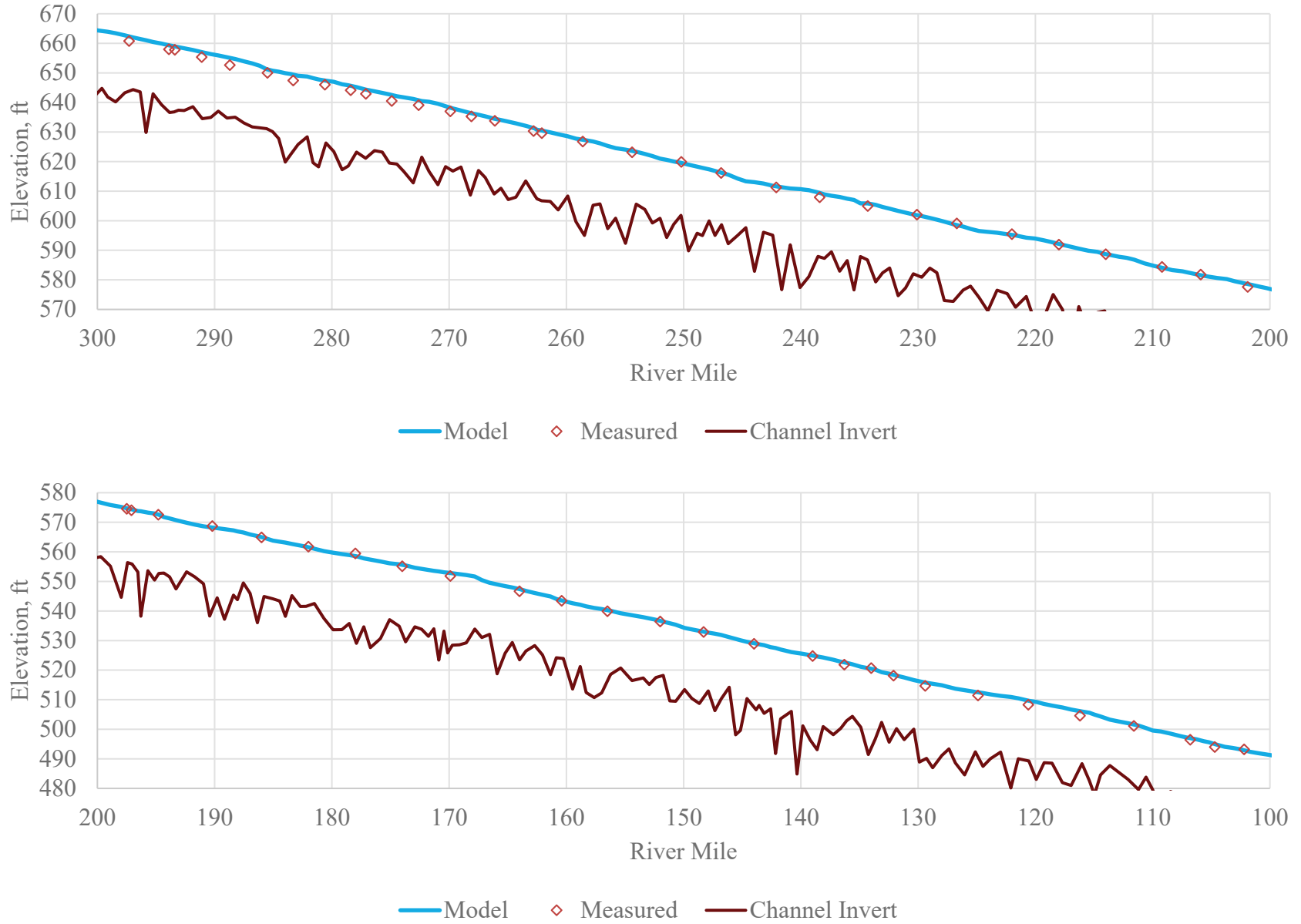


Figure 32. Model hydraulic comparison at low flow: River Miles 300 - 100

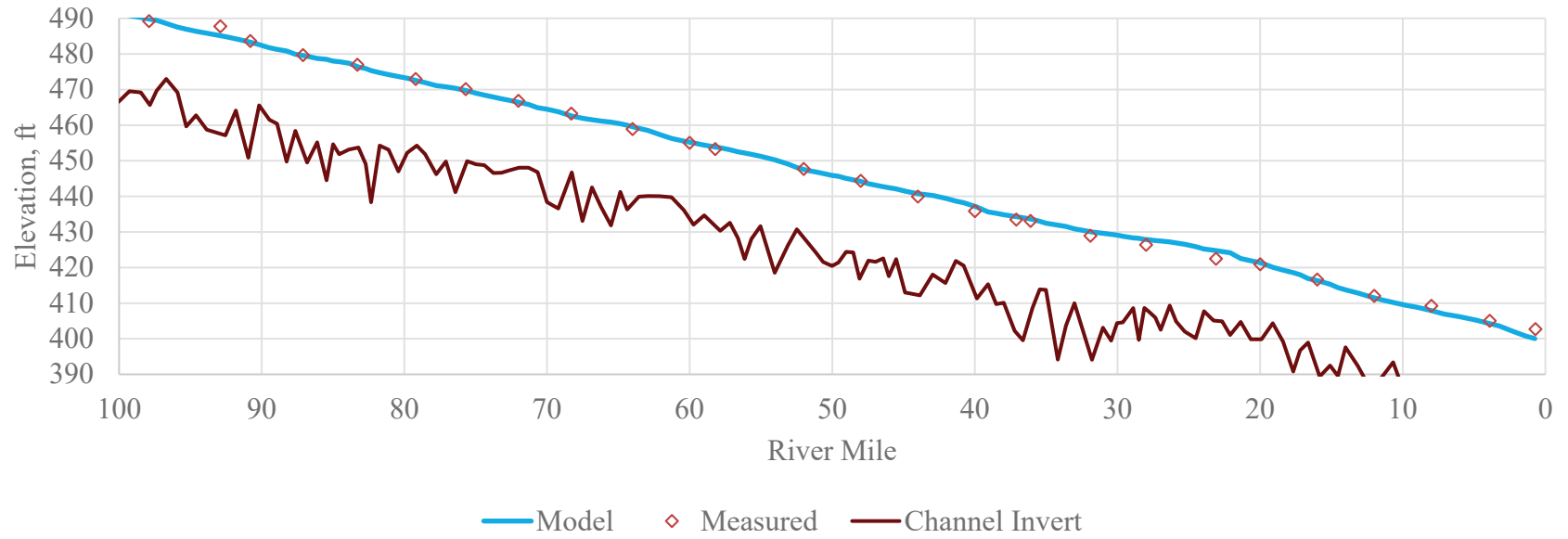


Figure 33. Model hydraulic comparison at low flow: River Miles 100 - 0

A moderately high flow event occurred within a year of the model start. Figures 34 – 39 compare model results to the water surface elevation at the USGS Missouri River gages at St. Joseph, Kansas City, Waverly, Boonville, Herman, and St. Charles, respectively.

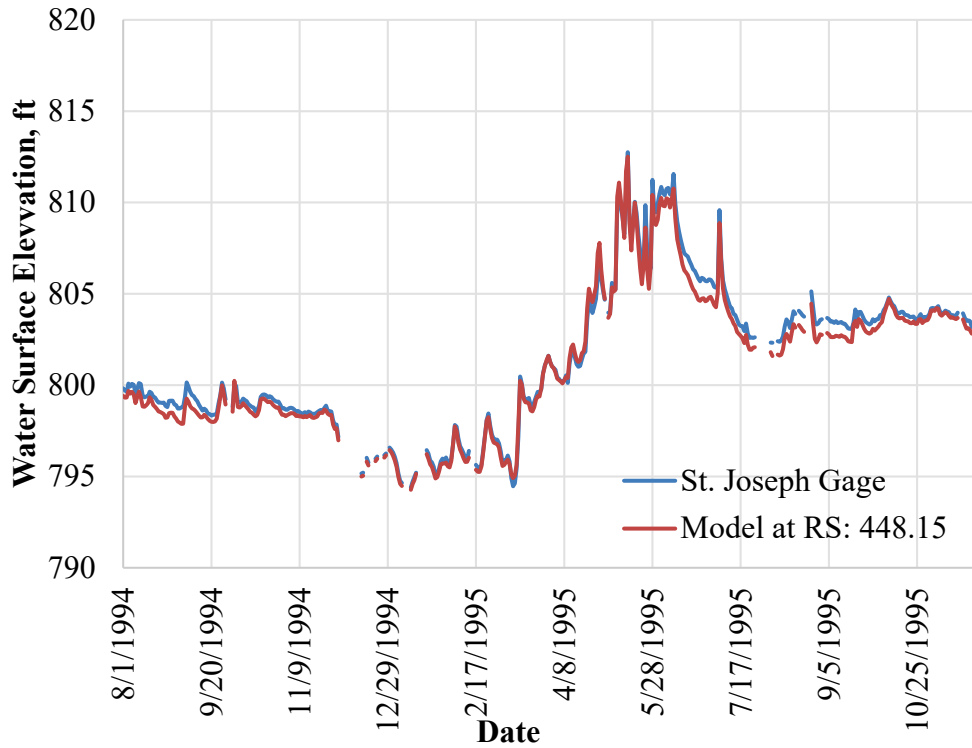


Figure 34. Water surface at the St. Joseph gage during first year of calibration period

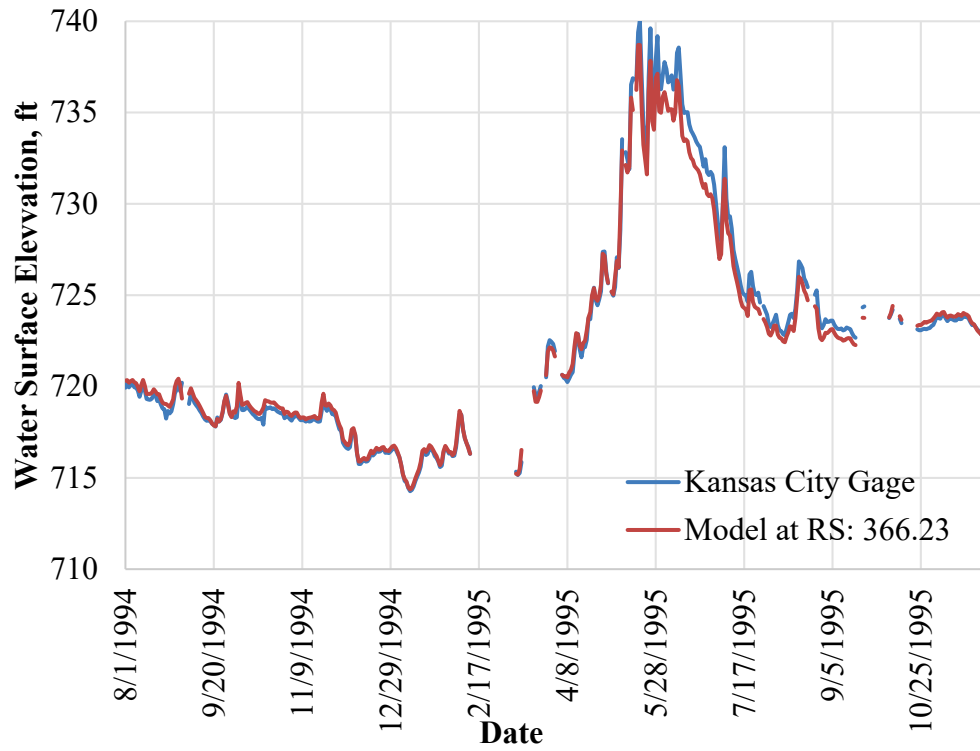


Figure 35. Water surface at the Kansas City gage during first year of calibration period

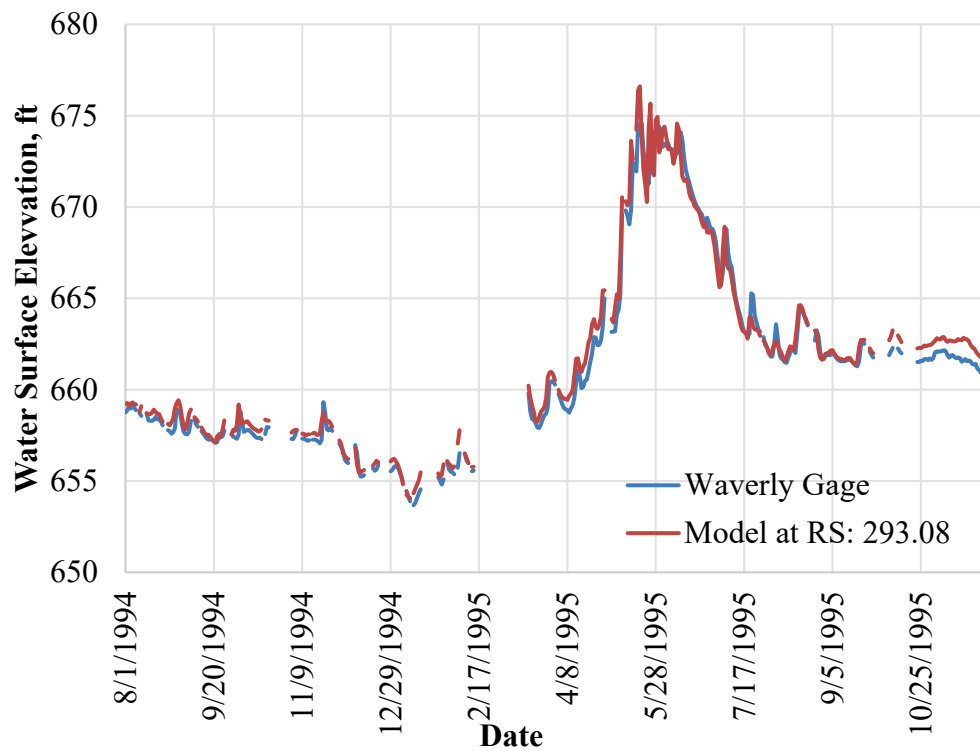


Figure 36. Water surface at the Waverly gage during first year of calibration period

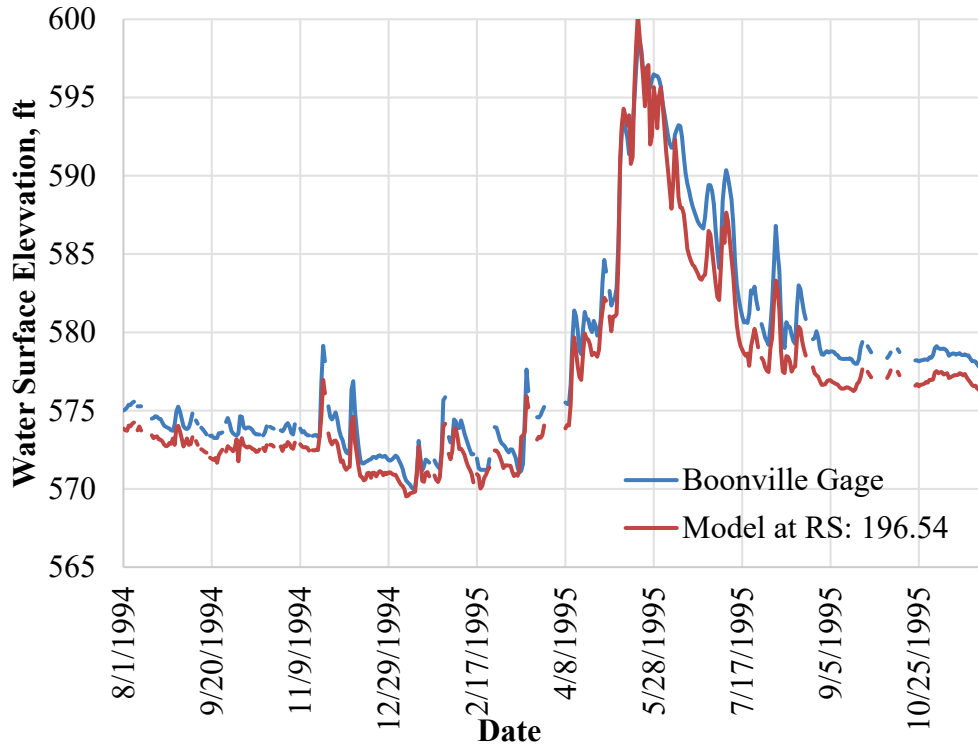


Figure 37. Water surface at the Boonville gage during first year of calibration period

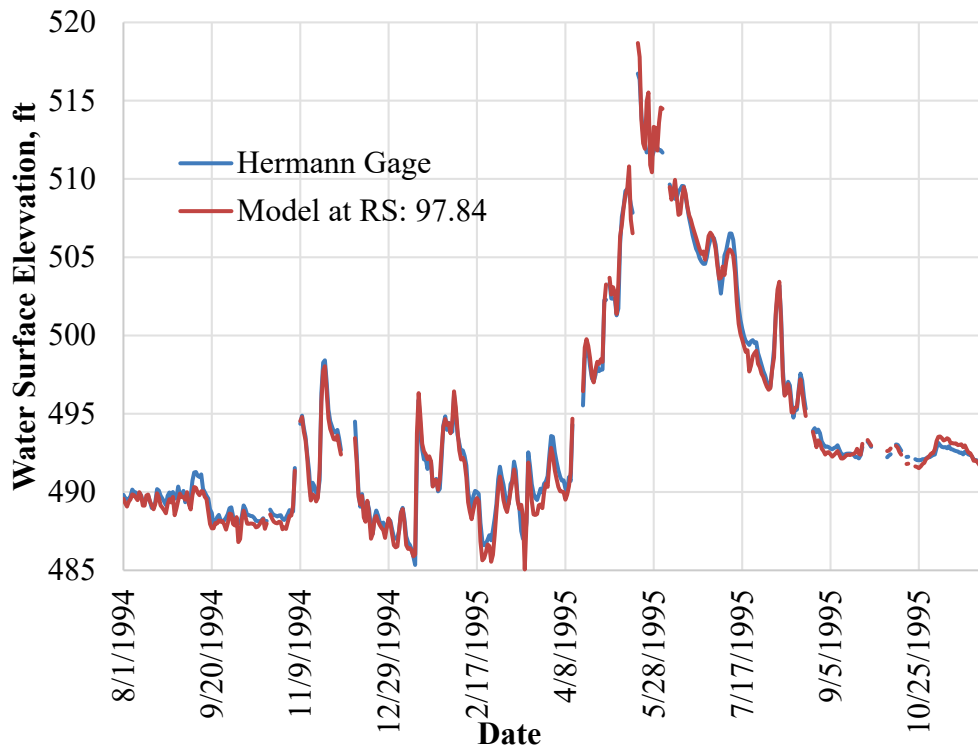


Figure 38. Water surface at the Hermann gage during first year of calibration period

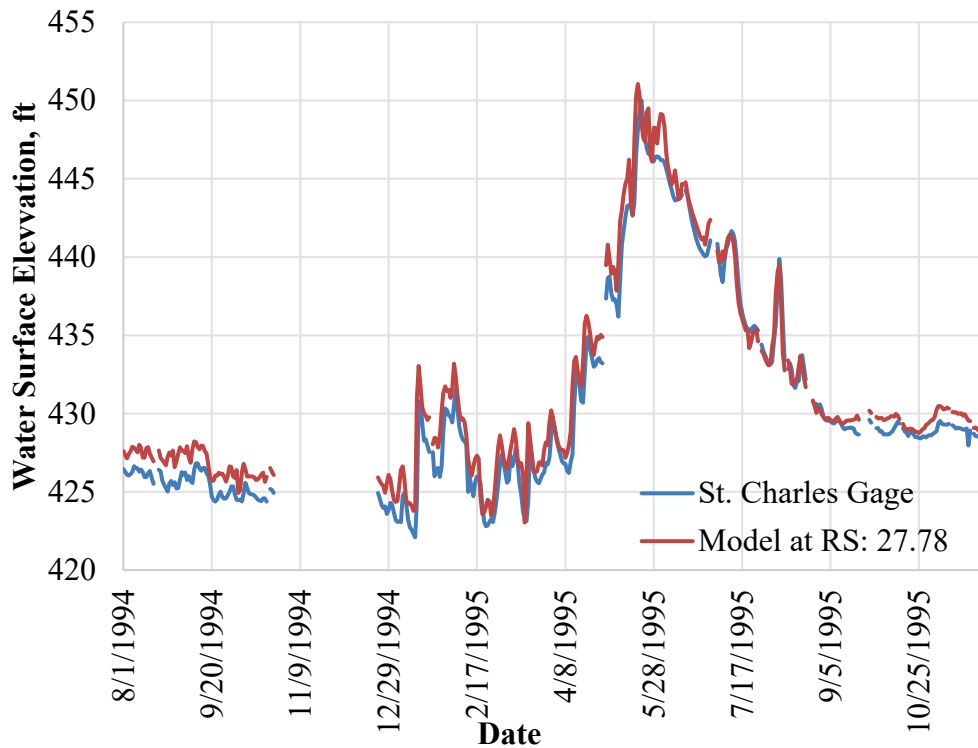


Figure 39. Water surface at the St. Charles gage during first year of calibration period

Output shown in Figures 34 to and 39 is from the mobile-bed model and therefore includes slight bed changes over the course of the first year. Table 19 provides the average absolute difference between the model and measured water surfaces. This is reasonable agreement, given the 498 mile length of this quasi-unsteady model. Attempts to reduce the discrepancy at Boonville were found to cause unreasonable departures in other calibration metrics.

Table 19. Average Absolute Departure from Daily Gage Measurements in the First Year of Simulation (ft)

SJ	KC	WV	BV	HR	SC
0.30	0.46	0.51	1.58	0.53	1.19

**Hydraulic Calibration- Long Term**

The agreement of the model water surface elevation over the full calibration period (1994 to 2014) is a verification of the temporal fidelity of the sediment modeling. Table 20 indicates small departures over the course of the 20-year simulation.

Table 20. Average Absolute Departure from Daily Gage Measurements over Full Calibration Period -- Aug 1994 to July 2014 (ft)

SJ	KC	WV	BV	HR	SC
-0.03	-0.70	0.15	-0.81	-0.18	0.12

**Velocity Calibration**

Channel velocities were measured during, soon after, and one year after the 2011 flood via ADCP. As seen in Figure 40, model velocities are in reasonable agreement with measured velocities. The measurements in July of 2012 purposefully measured locations with the greatest dike constriction, which explains some of the higher velocities.

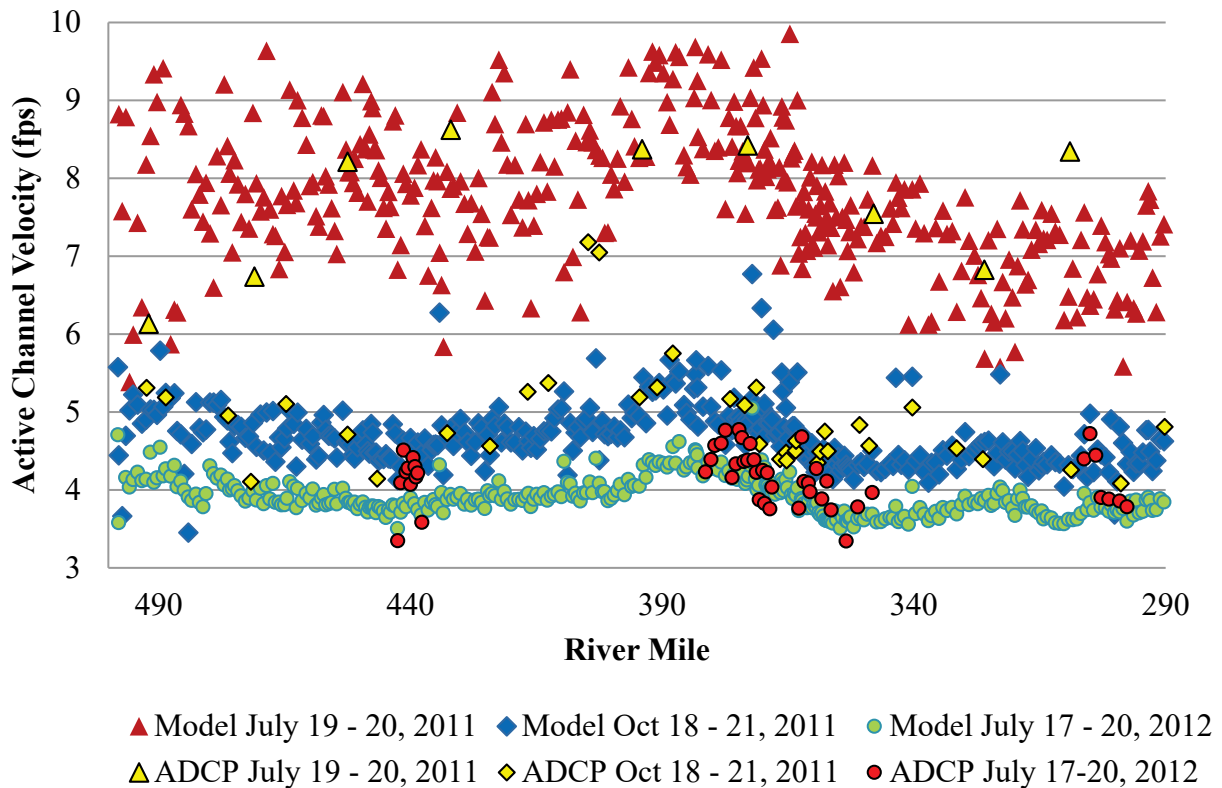


Figure 40. Velocity Comparison

**Sediment Load**

USGS (Heimann et al., 2010) provides an estimate for annual suspended sediment sand loads through water year 2005 at multiple gages on the Missouri River. Table 21 compares these suspended sediment values plus bedload values from rating curves developed from Abraham et al. (2017) against model values for sediment transport at the gages. The model output agrees quite well with the measured values and is well within the uncertainty estimates presented in (Heimann et al., 2010).

Table 21. Sediment Load Comparison from 01 Oct 1994 to 30 Sep 2005 at Mainstem Gages

Gage	Model	USGS+Bedload	Model/Measured
SJ	113,817,726	116,179,350	0.98
KC	140,280,159	141,362,547	0.99
HR	175,773,026	189,286,266	0.93

**Bed Elevation and Mass Calibration**

Figure 41 presents bed elevation change at each model cross-section and each measured location. As seen, the model accurately reproduces degradation trends, though both measured data and model output exhibit significant variability and scatter. The nature of the active bedforms on the Missouri River causes individual cross sectional measurements to vary by several feet even without persistent geomorphic change. USACE (2015) finds that 75% of cross sections varied 0.25 ft to 3 ft from 2008 to 2009, but some temporarily rose or fell by as much as 11 ft in a single year.

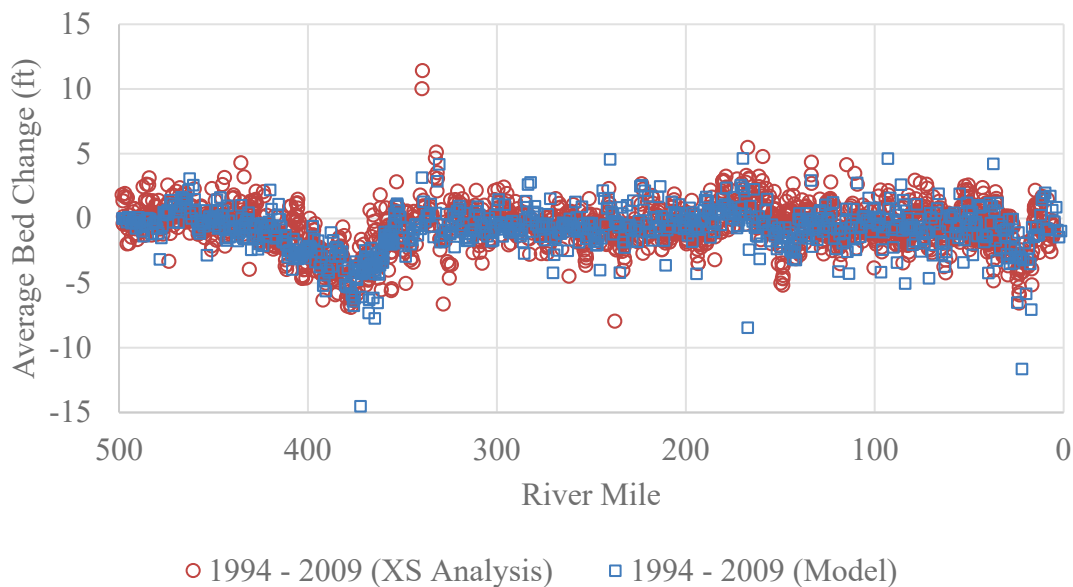


Figure 41. Model vs. Measured Bed Elevation Change 1994 to 2009

With a sufficient number of cross sections, these random fluctuations average out, which makes volume or mass change over reaches especially useful for comparing model to measured output rather than bed change at an individual cross section. Figure 42 plots the longitudinal cumulative mass change for both model and measured cross sections from 1994 to 2009. As seen in Figure 42, the calibrated model closely approximates the magnitude and location of mass change from 1994 to 2009. This time period includes both high flows and low flows and a range of channel mining rates and indicates the strength of the calibration for long-term modeling.

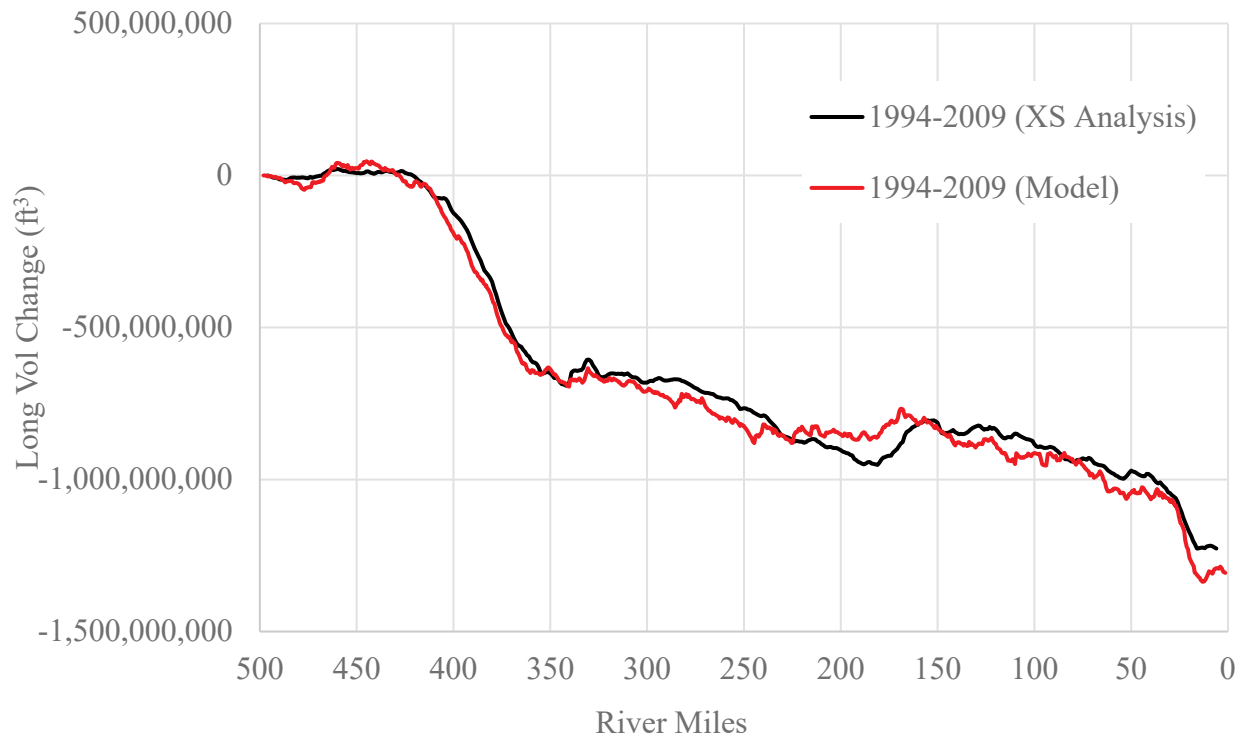


Figure 42. Longitudinal Cumulative Mass Calibration: 1994 to 2009

Figure 43 presents an initial longitudinal cumulative mass change from 2009 to 2014. The 2011 flood and post-flood rebound dominates the bed change over this time period. As seen, the model reasonably reproduced upstream headcut migration visible from RM 500 to aprx. RM 388, as well as the general degradation trend from RM 181 to RM 0. The model did not reproduce the rebound observed from RM 350 to 181. The cross section analysis (depicted in Figure 12) indicates that the sediment eroding from RM 500 to 388 did not simply redeposit downstream; from year 2009 to 2012 the headcut progressed upstream while the downstream channel was also erosional. The rebound occurred after the flood--from 2012 to 2013 and from 2013 to 2014. The mainstem and tributary rating curves developed from USGS data as used in this model do not bring in sufficient sediment to account for the post-flood rebound. Anecdotal evidence suggests that the source of the sediment may be eroding banks or headcutting up tributaries—but these sources have not been quantified.

Including an additional 23 million tons in sediment load from unknown sources following the 2011 event yields Figures 44 and 45. As seen, this provides a better estimate for the post-flood rebound following the 2011 event. To avoid negative bias in future projections, the 23M will be added in after a repeat of the 2011 event in the period of record. As Figure 12 does not indicate a similar rebound following the 1993 flood, the extra tonnage is not added following the 1993 flood or other floods in the projection period.

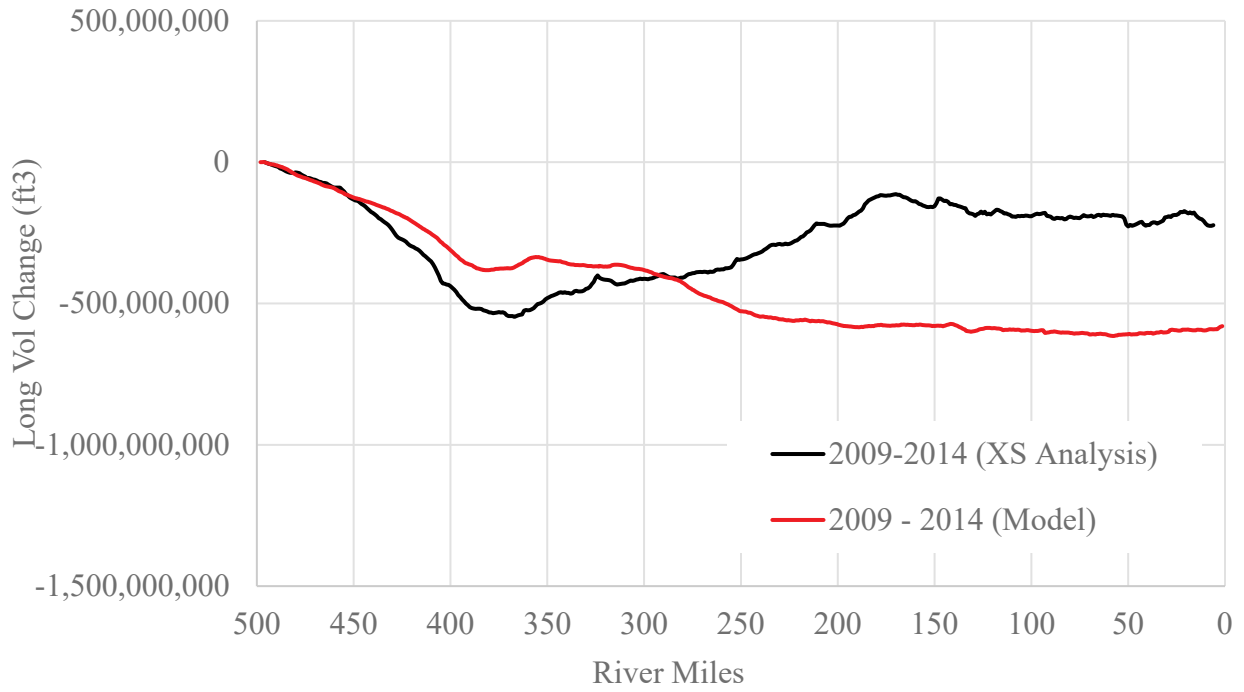


Figure 43. Longitudinal cumulative mass calibration: 2009 to 2014 with no additional post-2011 sediment

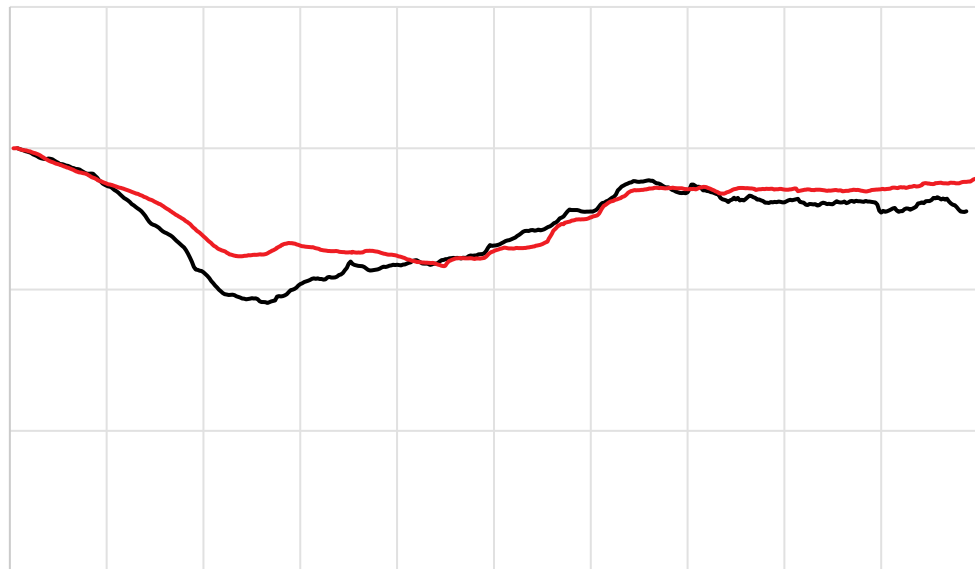


Figure 44. Longitudinal Cumulative Mass Calibration: 2009 to 2014 with additional 23M tons of post-2011 flood sediment

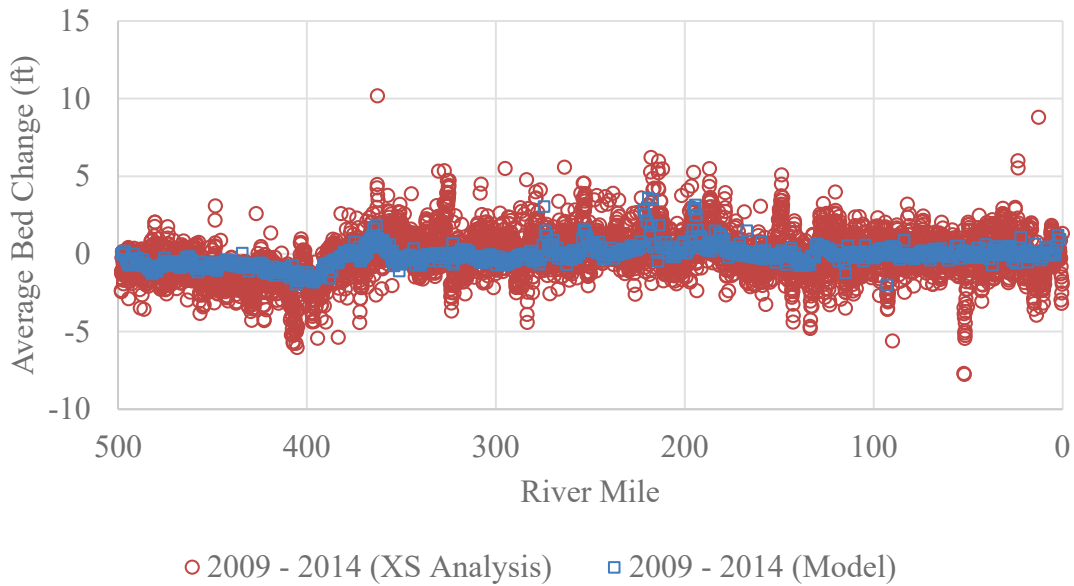


Figure 45. Model vs. Measured Bed Elevation Change 2009 to 2014. Model output includes 23M tons of post-2011 flood sediment.

### Conclusion

This report described the mobile-bed model developed for modeling bed change on the lower 500 miles off the Missouri River. It served as an orientation to the inputs, assumptions, and modeling choices that have occurred. The model outputs for water surface, velocity, sediment transport, bed elevation change, and bed volume change over the calibration period reasonably match the prototype using realistic initial conditions and boundary conditions and appropriate model parameters. The model has been calibrated to the Missouri River and is deemed suitable use in MRRP planning.

## References

- Abraham, D. Ramos-Villaneuva, M., Pratt, T., Ganesh, N., May, D., Butler, W., McAlpin, T., Jones, K., Shelley, J., and Pridal, D. (2017). Sediment and Hydraulic Measurements with Computed Bed Load on the Missouri River, Sioux City to Hermann, 2014. ERDC/CHL TR-17-8. U.S. Army Corps of Engineers, Engineering Research and Development Center, Coastal and Hydraulics Laboratory. Vicksburg, MS.
- Abraham, D., Kuhnle, R., and Odgaard, A. J., (2011), "Validation of Bed Load Transport Measurements with Time-Sequenced Bathymetric Data." *J. Hydr. Engrg.*, ASCE, 137(7), 723-728.
- Alexander, J.S., Jacobson, R.B., and Rus, D.L., 2013, Sediment transport and deposition in the lower Missouri River during the 2011 flood: U.S. Geological Survey Professional Paper 1798–F, 27 p., <http://dx.doi.org/10.3133/pp1798f>.
- HEC (1982). Guidelines for the Calibration and Application of Computer Program HEC-6. Hydrologic Engineering Center, U.S. Army Corps of Engineers. Davis, CA.
- HEC (2010). HEC-RAS Hydraulic Reference Manual. January 2010. Hydrologic Engineering Center, U.S. Army Corps of Engineers. Davis, CA.
- Heimann, D.C., Rasmussen, P.P., Cline, T.L., Pigue, L.M., and Wagner, H.R. (2010). Characteristics of sediment data and annual suspended-sediment loads and yields for selected lower Missouri River mainstem and tributary stations, 1976–2008: U.S. Geological Survey Data Series Report 530, 58 p.
- Horowitz, A.J. (2006). "The effect of the 'Great Flood of 1993' on subsequent suspended sediment concentrations and fluxes in the Mississippi River Basin, USA." *Sediment Dynamics and the Hydrogeomorphology of Fluvial Systems*. IAHS Publ. 306, 2006.
- Julien, P.Y. (1994). *Erosion and Sedimentation*, Cambridge University Press, QE571.J85, ISBN 0-521-44237-0 Hardback in 1995, Paperback in 1998, 280p.
- Laustrup, M.S., Jacobson, R.B., and Simpkins, D.G. (2007). Distribution of potential spawning habitat for sturgeon in the Lower Missouri River: U.S. Geological Survey Open-File Report 2007-1192, 26 p.
- MoDOT (2008). Missouri Highways and Transportation Commission Plans for Proposed Interstate Highway I-29/35, Clay-Jackson Counties, River Bridge Segment, River Bridge Plans. The kcION Project, Paseo Corridor Constructors. Kansas City, MO.
- SCS (1993). Impacts of the 1993 Flood on Missouri's Agricultural Land. U.S. Department of Agriculture, Soil Conservation Service. October 1993.

Shelley, J., Abraham, D., and McAlpin, T. (2013). "Removing Systemic Bias in Bed-Load Transport Measurements in Large Sand-Bed Rivers." *J. Hydraul. Eng.*, 0.1061/(ASCE)HY.1943-7900.0000760 (Mar. 22, 2013). [http://ascelibrary.org/doi/abs/10.1061/\(ASCE\)HY.1943-7900.0000760](http://ascelibrary.org/doi/abs/10.1061/(ASCE)HY.1943-7900.0000760)

Simons, Li & Associates (1982). *Engineering Analysis of Fluvial Systems*. Fort Collins, CO.

USACE (1981). *Missouri River Bank Stabilization and Navigation Project Final Feasibility Report and Final EIS for the Fish and Wildlife Mitigation Plan*. U.S. Army Corps of Engineers, Missouri River Division.

USACE (1994). *Missouri River Hydrographic Survey: Rulo, Nebraska to the Mouth*. U.S. Army Corps of Engineers, Kansas City District. Kansas City, MO.

USACE (2006). *Missouri River Mainstem Reservoir System, Master Water Control Manual, Missouri River Basin*. Reservoir Control Center, U. S. Army Corps of Engineers, Northwestern Division - Missouri River Basin, Omaha, Nebraska. Revised March 2006. <http://www.nwd-mr.usace.army.mil/mmanual/mast-man.htm>.

USACE (2007). *Calibrating a HEC-RAS Model of the Missouri River for FEMA Floodway Development*. <http://www.nwd-c.usace.army.mil/PB/HHCOP/MO%20R%20FLOODWAY.pdf>.

USACE (2009). *Missouri River Bed Degradation Reconnaissance Study Section 905(b) (Water Resources Development Act of 1986) Analysis*. U.S. Army Corps of Engineers, Kansas City District. Kansas City, MO.

USACE (2010). *Memorandum for Record: Documentation of Missouri River Low Water Surface Profile Adjustment Procedure*. U.S. Army Corps of Engineers, Kansas City District. Kansas City, MO.

USACE (2011). *Missouri River Commercial Dredging Final Environmental Impact Statement*. U.S. Army Corps of Engineers, Kansas City District. Kansas City, MO. Prepared by Cardno-Entrix, Seattle, WA.

USACE (2017a). *Missouri River Bed Degradation Feasibility Study Technical Report*. U.S. Army Corps of Engineers, Kansas City District.

USACE (2017b). *Missouri River Stage Trends Technical Report, September 2017*. U.S. Army Corps of Engineers, Missouri River Basin Water Management Division. Omaha, NE. <http://www.nwd-mr.usace.army.mil/rcc/reports/pdfs/MRStageTrends2017.pdf>